



**THESIS APPROVAL**  
**GRADUATE SCHOOL, KASETSART UNIVERSITY**

Master of Science (Biotechnology)

**DEGREE**

Biotechnology

Biotechnology

**FIELD**

**DEPARTMENT**

**TITLE:** Isolation and Characterization of Nanocellulose from Mango and Rambutan Peels Obtained By Steam Explosion Combined With Chemical Treatments

**NAME:** Mr. Naiyasit Yingkamhaeng

**THIS THESIS HAS BEEN ACCEPTED BY**

**THESIS ADVISOR**

( Mr. Prakit Sukyai, Dr. nat. techn. )

**DEPARTMENT HEAD**

( Assistant Professor Suttipun Keawsompong, Ph. D. )

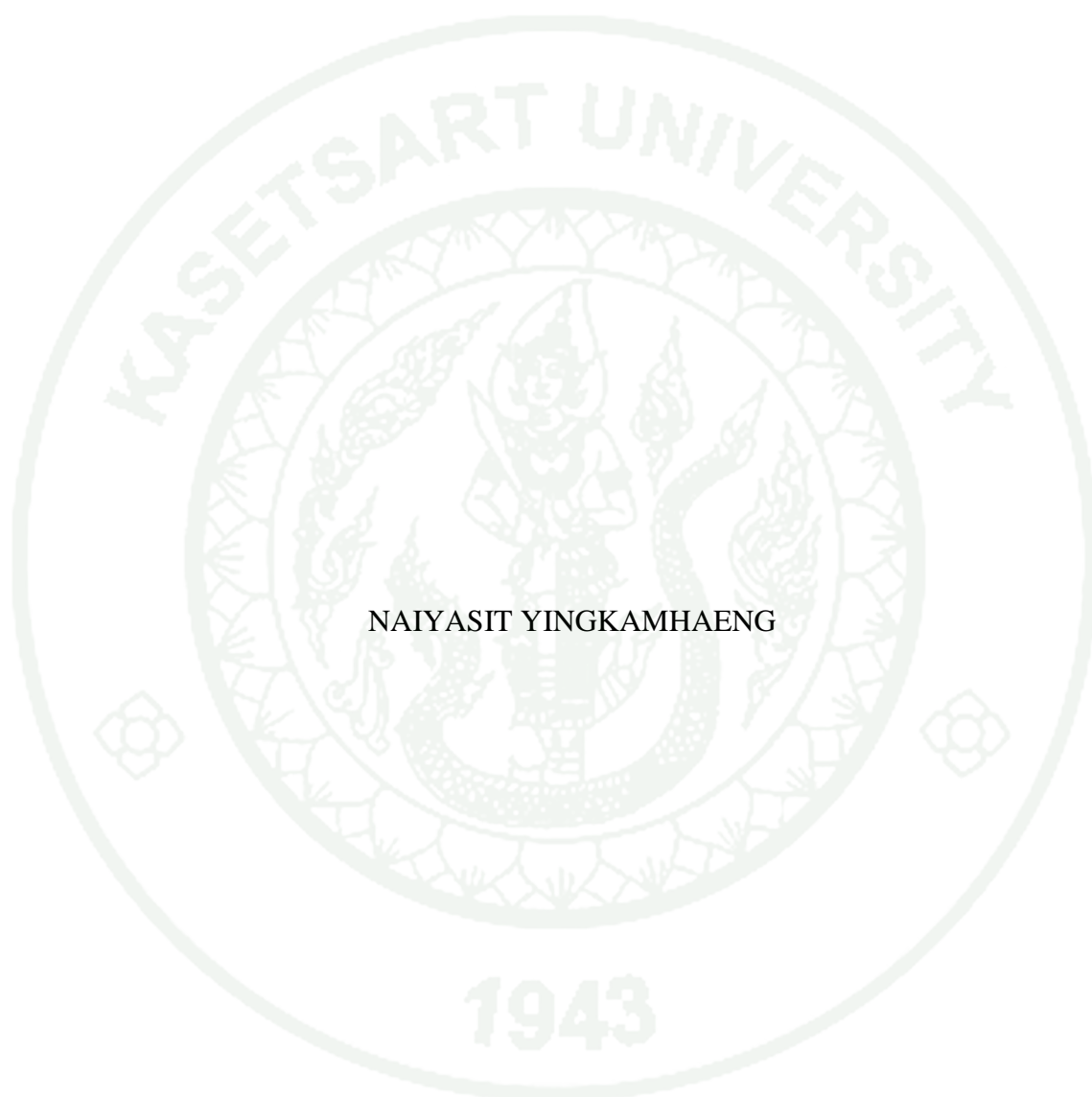
**APPROVED BY THE GRADUATE SCHOOL ON**

**DEAN**

( Associate Professor Gunjana Theeragool, D.Agr. )

THESIS

ISOLATION AND CHARACTERIZATION OF NANOCELLULOSE  
FROM MANGO AND RAMBUTAN PEELS OBTAINED BY STEAM  
EXPLOSION COMBINED WITH CHEMICAL TREATMENTS



NAIYASIT YINGKAMHAENG

A Thesis Submitted in Partial Fulfillment of  
the Requirements for the Degree of  
Master of Science (Biotechnology)  
Graduate School, Kasetsart University  
2014

Naiyasit Yingkamhaeng 2014: Isolation and Characterization of Nanocellulose from Mango and Rambutan Peels Obtained by Steam Explosion Combined with Chemical Treatments. Master of Science (Biotechnology), Major Field: Biotechnology, Department of Biotechnology. Thesis Advisor: Mr. Prakrit Sukyai, Dr.nat.techn. 72 pages.

The aim of this work is to isolate nanocellulose from mango and rambutan peels that abundantly found in food processing industries in Thailand. The environmentally friendly uncatalyzed steam explosion combined with bleaching treatment was used for nanocellulose extraction. The chemical composition of fibers in different processing stages revealed the  $\alpha$ -cellulose content from mango and rambutan peels increased to 94% and 81%, respectively, while hemicellulose and lignin content were significantly decreased during extraction processes. It was found that those methods showed great potential for removing of hemicellulose and lignin. The scanning electron microscopy (SEM) and fourier transform infrared (FTIR) spectroscopy analysis were used to confirm the removal of lignin and hemicellulose in their components. Atomic force microscopy (AFM) analysis was utilized to support that obtainable nanocellulose in both raw fibers exhibited rod-like shape and the size of fibers showed a relative uniform size with length and width of below 200 nm and around 5-40 nm, respectively. The crystallinity of fibers was determined by X-ray diffraction (XRD) method which displayed the increase of crystallinity of nanocellulose comparing with raw fibers. Thermogravimetric analysis (TGA) found that nanocellulose from rambutan peel presented higher thermal stability (329 °C) comparing to nanocellulose from mango peel (265 °C). This indicated that cellulose source has an effect on the nanocellulose properties. We hope that in this study will be used as a model for nanocellulose investigation from other lignocellulosic materials.

---

Student's signature

---

Thesis Advisor's signature

\_\_\_ / \_\_\_ / \_\_\_

## ACKNOWLEDGEMENTS

I would like to express my gratitude to my thesis advisor Dr. Prakrit Sukyai for his kind encouragement and for helpfulness, guidance, improvement throughout this work.

I would like to thank also Chantaburi Global Trade Co., Ltd., Chantaburi, Thailand for kindly provided the mango peel sample.

I would like to place on record my great appreciation to all Department of Biotechnology members and my colleagues who help throughout my study.

I would like to thank to Kasetsart University Research and Development Institute (KURDI) who supported the great throughout this research.

Finally, I am especially appreciated my mother Mrs. Vilaiwan Yingkamhaeng and my family for their containing encouragements.

Naiyasit Yingkamhaeng  
December, 2014

**TABLE OF CONTENTS**

	<b>Page</b>
TABLE OF CONTENTS	i
LIST OF TABLES	ii
LIST OF FIGURES	iii
LIST OF ABBREVIATIONS	vi
INTRODUCTION	1
OBJECTIVES	4
LITERATURE REVIEW	5
MATERIALS AND METHODS	25
Materials	25
Methods	26
RESULTS AND DISCUSSION	31
CONCLUSION	63
LITERATURE CITED	64
CURRICULUM VITAE	72

**LIST OF TABLES**

<b>Table</b>		<b>Page</b>
1	Chemical composition of some typical cellulose-containing materials	6
2	Type of nanocellulose	11
3	Various natural fibers for isolation of nanocellulose	12
4	Various processes used for isolation of nanocellulose	19
5	Chemical composition of mango peel in different treatments	33
6	Chemical composition of rambutan peel in different treatments	33
7	The dominant peak absorption of mango peel in different fibers	48
8	The dominant peak absorption of rambutan peel in different fibers	49
9	Crystallinity index (CrI) of mango and rambutan peels at different stages of treatment	54
10	Thermal behavior of untreated and treated mango peel fibers	57
11	Thermal behavior of untreated and treated rambutan peel fibers	59
12	Degradation characteristic of bleached fibers and acid-hydrolyzed fibers in mango and rambutan peels	62

## LIST OF FIGURES

<b>Figure</b>		<b>Page</b>
1	Cellulose microfibrils from various sources in nature	5
2	Basic chemical structure of cellulose showing the cellulosic repeat unit ( $n = DP$ , degree of polymerization)	8
3	Relationships of the different cellulose allomorphs and some prototypical fibers diffractograms	9
4	Schematic of the tree hierarchical structure	12
5	Schematic diagram of the physical structure of a semi-crystalline cellulose fibers	13
6	Scheme of main steps needed to prepare nanocellulose from lignocellulosic biomass (NC = nanocellulose)	14
7	Schematic presentation of effects of pretreatment on lignocellulosic biomass	17
8	Acid hydrolysis mechanism (a) and esterification of cellulose nanocrystals surfaces (b)	20
9	Photographs of steam explosion at Kasetsart Agricultural and Agro-Industrial Product Improvement Institute (KAPI)	29
10	Scheme for nanocellulose production from mango and rambutan peels	30
11	Bleaching at different processing stages; one time (a), two times (b), three times (c), four times (d), five times (e) and six times (f)	36
12	Photographs of mango peel; untreated fibers (a), steam-exploded fibers (b) and bleached fibers (c).	37
13	Scanning electron micrograph of mango peel; untreated fibers (a), steam-exploded fibers (b) and bleached fibers (c)	39
14	Scanning electron micrograph of rambutan peel; untreated fibers (a), steam-exploded fibers (b) and bleached fibers (c)	40

## LIST OF FIGURES (Continued)

<b>Figure</b>		<b>Page</b>
15	AFM photograph of nanocellulose from mango peel; height image (a) and phase image (b)	43
16	AFM photograph of nanocellulose from rambutan peel; height image (a) and phase image (b)	44
17	Height distribution of diluted nanocellulose (0.01 mg/ml) from mango peel (a) and rambutan peel (b) analyzed by Gwyddion program	45
18	FTIR spectra of mango peel; untreated fibers (a), steam-exploded fibers (b), bleached fibers (c) and acid-hydrolyzed fibers (d)	47
19	FTIR spectra of rambutan peel; untreated fibers (a), steam-exploded fibers (b), bleached fibers (c) and acid-hydrolyzed fibers (d)	47
20	X-ray diffraction patterns of mango peel; untreated fibers (a), steam-exploded fibers (b), bleached fibers (c) and acid-hydrolyzed fibers (d)	53
21	X-ray diffraction patterns of rambutan peel; untreated fibers (a), steam-exploded fibers (b), bleached fibers (c) and acid-hydrolyzed fibers (d)	53
22	TG curves of mango peel; untreated fibers (a), steam-exploded fibers (b), bleached fibers (c) and acid-hydrolyzed fibers (d)	56
23	DTG curves of mango peel; untreated fibers (a), steam-exploded fibers (b), bleached fibers (c) and acid-hydrolyzed fibers (d)	56
24	TG curves of rambutan peel; untreated fibers (a), steam-exploded fibers (b), bleached fibers (c) and acid-hydrolyzed fibers (d)	58
25	DTG curves of rambutan peel; untreated fibers (a), steam-exploded fibers (b), bleached fibers (c) and acid-hydrolyzed fibers (d)	58
26	The thermal degradation of bleached fibers (cellulose microfibers) from mango (a) and rambutan peels (b)	62

**LIST OF FIGURES (Continued)**

<b>Figure</b>		<b>Page</b>
27	The thermal degradation of acid-hydrolyzed fibers from mango (a) and rambutan peels (b)	64



## LIST OF ABBREVIATIONS

TEMPO	=	2,2,6,6-tetramethylpiperidine-1-oxyl
ASTM	=	American Society for Testing and Materials
AFM	=	Atomic force microscopy
BC	=	Bacterial cellulose
cm	=	centimeter
CrI	=	Crystallinity Index
$\epsilon_B$	=	Elongation at break
$^{\circ}\text{C}$	=	degree Celsius
DP	=	degree of polymerization
DSC	=	Differential Scanning Calorimetry
DTA	=	Differential Thermogravimetric Analysis
DMSO	=	dimethylsulfoxide
DLS	=	Dynamic light scattering
FTIR	=	Fourier Transform Infrared Spectroscopy
$T_g$	=	Glass-rubber transition Temperature
g	=	gram
h	=	hour
HCl	=	hydrochloric acid
$T_m$	=	Melting Temperature
$\mu\text{m}$	=	micrometer
mg	=	milligram
ml	=	milliliter
min	=	minute
NCF	=	nanocellulose fibers
nm	=	nanometer
$T_o$	=	Onset temperature
PC	=	plant cellulose
PHA	=	poly(hydroxyalkanoate)
PLA	=	poly(lactic acid)

**LIST OF ABBREVIATIONS (Continued)**

KBr	=	potassium bromide
rpm	=	round per minute
SEM	=	Scanning Electron Microscopy
sec	=	second
NaOH	=	sodium hydroxide
xg	=	times gravity
$\sigma$	=	Tensile strength
TGA	=	Thermogravimetric Analysis
TPS	=	Thermoplastic starch
TEM	=	Transmission Electron Microscopy
v/v	=	volume/volume
H <sub>2</sub> O	=	water
w/v	=	weight/volume
w/w	=	weight/weight
XRD	=	X-ray diffraction
<i>E</i>	=	Young's module

# ISOLATION AND CHARACTERIZATION OF NANOCELLULOSE FROM MANGO AND RAMBUTAN PEELS OBTAINED BY STEAM EXPLOSION COMBINED WITH CHEMICAL TREATMENTS

## INTRODUCTION

In recent years, environmental awareness has become a major issue and the demand for new green materials able to replace materials based on fossil resources has constantly been growing. Research for development of biodegradable materials from renewable sources is increasing. The availability of biopolymers, relatively cheaper, which occur in abundance in nature, can be cited as an important reason (Cherian *et al.*, 2011).

Cellulose is one of renewable biopolymers, which abundantly found in nature (Morán *et al.*, 2008). It has gained important for a widely applications, such as paper and pulp industries, food packaging, medical materials, reinforcing and composites (Siqueira *et al.*, 2010; Klemm *et al.*, 2011; Johar *et al.*, 2012; Khalil *et al.*, 2012). However, in order to efficiently utilize cellulose as raw materials in emerging bio-based applications the cellulose nanofibers are extensively applied. The nano-dimensions of the structure resulting in exhibited the potential properties (Klemm *et al.*, 2011), which enable a range of potential applications. Therefore, there is the growing research about nanocellulose increasing, such as good mechanical properties (Rosa *et al.*, 2010), high surface area (Chen *et al.*, 2011), low coefficient of thermal expansion (Bondeson *et al.*, 2006; Kaushik *et al.*, 2010) and biodegradability (Klemm *et al.*, 2011). Hence, there are the growing in the research of nanocellulose in order to created and developed a new bio-based materials that replace the petroleum-based materials (Brito *et al.*, 2012). One of most widely applications, nanocellulose play act as reinforcing filler in “green” nanocomposites (Lu and Hsieh, 2012) in the several polymer matrix, such as polyurethane (Cherian *et al.*, 2011), poly(vinyl) alcohol (Lee *et al.*, 2009), thermoplastic starch (Teixeira *et al.*, 2009; Kaushik *et al.*, 2010) and natural rubber (Pasquini *et al.*, 2010). The use of nanocellulose reinforcement aimed

to improve these polymers properties, such as tensile properties, compared to native polymers.

Plant based nanocellulose have growing research for preparing nanocellulose. The agricultural waste residues have been growing more attention in many researchers, which play acts as the main cellulose source due to its low cost and easy available. For example, sugarcane bagasse (Mandal and Chakrabarty, 2011) , coconut husk (Rosa *et al.*, 2010), cotton (Morais *et al.*, 2013), rice husk (Johar *et al.*, 2012) and sisal fibers (Morán *et al.*, 2008). In plant cells, cellulose fibers embedded in the lignocellulosic matrix such as lignin and hemicellulose as well as other polysaccharides (Klemm *et al.*, 2005). Hence, several cellulose extraction methods used to remove the non-cellulosic compounds, to obtain the highly purified cellulose. Extraction methods based chemical solvents are the most widely used. Although, a numerous studies have been studied the cellulose isolation based on chemical methods before nanocellulose isolation processes, which generate the chemical solvent wastes during extraction processes. Therefore, environmental friendly methods have been investigated for cellulose extraction from renewable resources.

Steam explosion is one of the environmental friendly extraction method (Abraham *et al.*, 2013) ,which is hydro-thermal methods involved high temperature and high pressure. During steam explosion, the steaming led to hemicellulose hydrolyzed and partially depolymerized of lignin (Deepa *et al.*, 2011). Then, the rapid release the pressure, resulting in the water explodes out the biomass caused the substance is rupture (Cherian *et al.*, 2011; Deepa *et al.*, 2011; Kaushik and Singh, 2011). This method is widely used to combination with other extraction methods to produce the highly purified cellulose and to reduce the use of hazard solvents (Jiang *et al.*, 2011), which in significantly lower environmental impact.

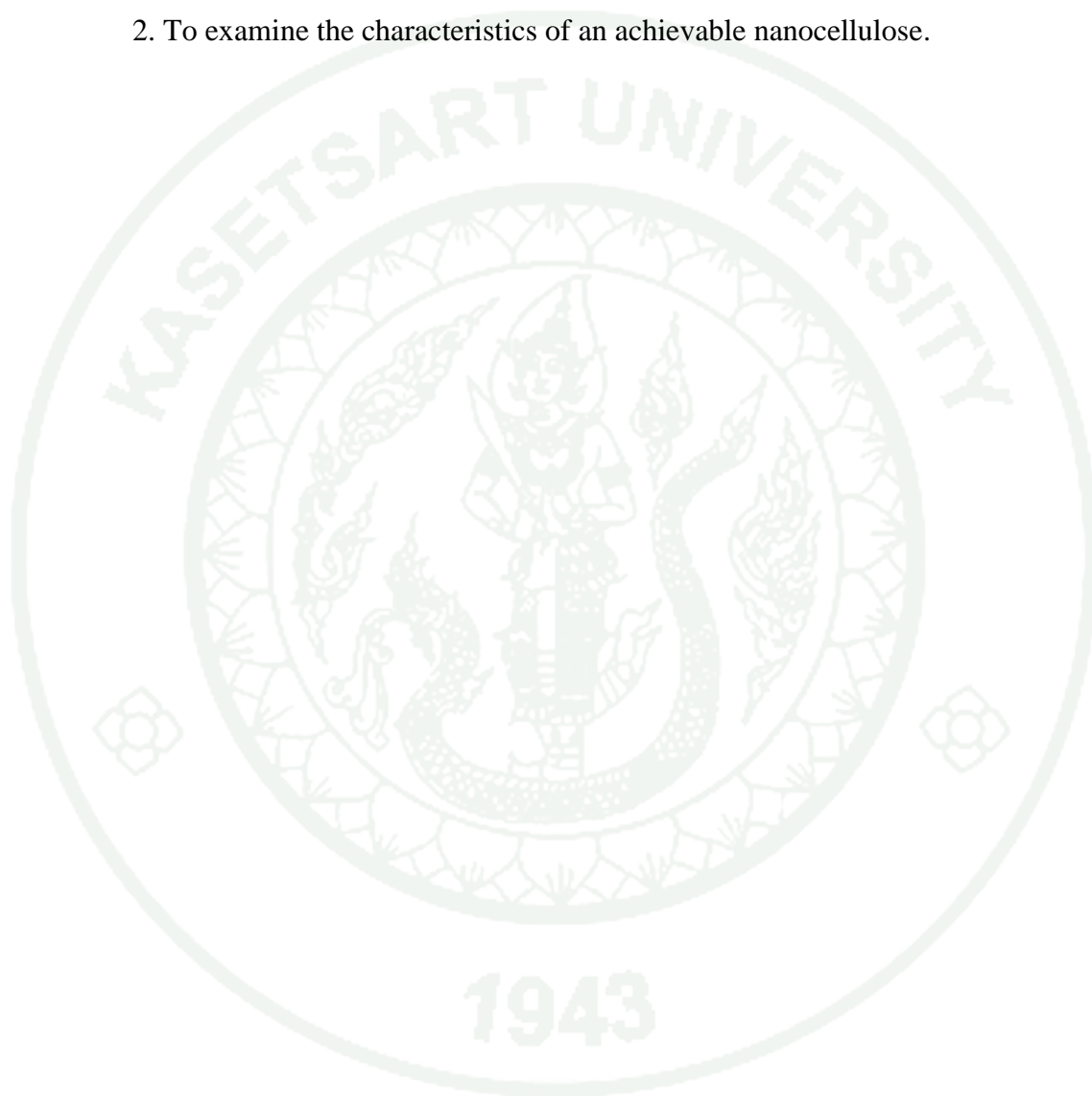
Mango and rambutan are a fruit that grow in almost all tropical regions of the world. Peel is a major waste obtained during processing of mango and rambutan production, which is constitutes about 15-20% of total weight (Ajila *et al.*, 2013). The chemical compositions of mango and rambutan peels have cellulose as main component. Thus, the utilization of mango and rambutan peels could be creating a

new cellulose sources. Therefore, this work is aimed to employ the mango and rambutan peels for the production of nanocellulose obtained by steam explosion combined bleaching treatments.



## OBJECTIVES

1. To investigate the utilization of mango and rambutan peels for nanocellulose extraction by using steam explosion combined with chemical processes.
2. To examine the characteristics of an achievable nanocellulose.



## LITERATURE REVIEW

### Cellulose

#### 1. Source

Cellulose is one of biopolymers, which is most abundantly found in nature, such as plants, animals, algae, as well as microbes, their properties and structure of cellulose depend on sources (Siqueira *et al.*, 2010). Generally, cellulose can be found in many forms and the most cellulose form in nature is plant cell wall, which has cellulose as main components (Zuluaga *et al.*, 2007). Figure 1 showed that cellulose fiber obtained from various sources and existing in nature in two native forms. The first is called complex cellulose that most of the celluloses present in nature and as component of the plant cell wall. The second is called pure cellulose, which presented in algae, some animals as well as it can be synthesized by some microorganisms (Pecoraro *et al.*, 2007; Liu and Sun, 2010).

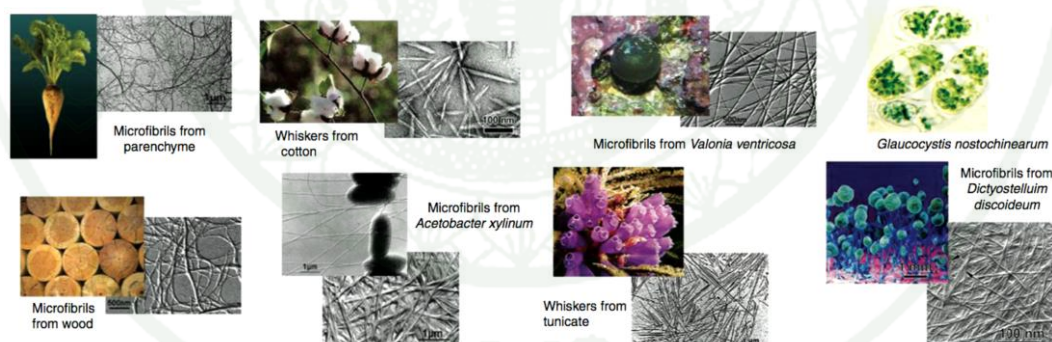


**Figure 1** Cellulose microfibrils from various sources in nature.

**Source:** Perez and Samain (2010)

#### 1.1 Plant cell wall

Plant cell wall is complex structure constituted of cellulose, hemicellulose and lignin, called lignocellulosic compound (Yu *et al.*, 2006) and may be composed

of other polysaccharides such as chitin, mannan and pectin, which are various in different kind of plant species. The main components of plant cell wall is cellulose, which is approximately 20-30% on dry weight basis (Perez and Samain, 2010). A major function of cell wall is to provide maintainable and support cell shape, mechanical strength, physical barrier and act as barrier to potential pathogens (Liu and Sun, 2010). The chemical composition of natural fibers varies according to their origin as summaries in Table 1.

**Table 1** Chemical composition of some typical cellulose-containing materials.

Source	Composition (%)			
	Cellulose	Hemicellulose	Lignin	Extract
Hardwood	43-47	25-35	16-24	2-8
Softwood	40-44	25-29	25-31	1-5
Coir	32-33	10-20	43-49	4
Corn cobs	45	35	15	5
Corn stalks	35	25	35	5
Cotton	95	2	1	0.4
Hemp	70	22	6	2
Kenaf	36	21	18	2
Ramie	76	17	1	6
Sisal	73	14	11	2
Wheat straw	30	50	15	5

**Source:** Adapted from Khalil *et al.* (2012)

## 1.2 Bacterial cellulose (BC)

Bacterial cellulose (BC) is synthesized by many genera such as, *Gluconacetobacter* sp., *Acetobacter xylinum*, *A. pasteurianus*, *A. hansenii*, *A. sucrofermantans* and *A. acetigenum*. The biosynthesis of bacterial cellulose shows splendid properties such as from high purity, highly crystalline and greater surface

area. Bacterial cellulose is used in many medical and industrial applications such as medical implants, coating, adhesives and composites (Cherian *et al.*, 2010). The production of bacterial cellulose by fermentation has two alternatives that are static culture and agitated culture, which also effect on the structure and properties of obtainable cellulose. In case of static culture, cellulose structure is showed in a pellicle form while, obtainable cellulose from agitated culture is in granule or fibrous form. Therefore, the industrial production of cellulose is based on plant cellulose. However, it is due to bacterial cellulose is expensive and there are many effects of culture condition on bacteria cellulose such as aging, carbon sources, bacterial species, as a result of the limitations in large-scale (Klemm *et al.*, 2005; Pecoraro *et al.*, 2007).

## 2. Structural and properties

Cellulose can be described as a homopolymer, consists of a linear polysaccharides composed of  $\beta$ -D-glucopyranose units linked by  $\beta$ -1,4-linkages. The basic structure of cellulose is shown in Figure 2. The non-etherified anomeric C1-OH is potential aldehyde and is known as the reducing end-group. The terminal glucopyranose residue with a free C4-OH is termed the non-reducing end group. Each structural unit has one primary OH group and two secondary OH groups, which act as chemical reactions (e.g. esterification). The length of cellulose chain has varies according to the sources of cellulose or each species of plants (Siqueira *et al.*, 2010).

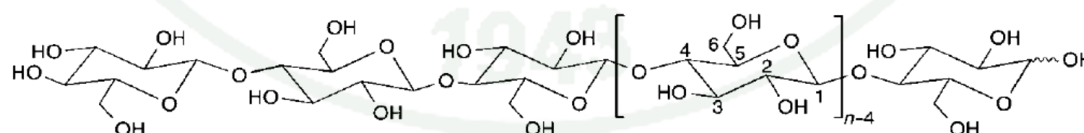


**Figure 2** Basic chemical structure of cellulose showing the cellulosic repeat unit ( $n =$  DP, degree of polymerization).

**Source:** Klemm *et al.* (2005)

The structure of cellulose chain has three hydroxyl groups located at C-2, at C-3 and at C-6 and each hydroxyl group linked together by hydrogen bond. Since, hydrogen bonding occurs in cellulose chain (intra- and intermolecular) resulting cellulose chain form become cellulose microfibrils that is two regions as crystalline region and amorphous region (Liu and Sun, 2010) and many cellulose microfibrils fuse become cellulose fibrils. Finally, cellulose chains are linked by hydrogen bond become cellulose fibers. Cellulose can be used to produce a broad variety of products obtained by chemical modification such as methylation, esterification, sulphonation, nitration and deoxyamination (Belgacem *et al.*, 2008). Therefore, there are many researchers have been studied to develop the properties of cellulose for suitable applications. On the basic of their X-ray patterns obtained from X-ray diffraction (XRD) and  $^{13}\text{C}$ -nuclear magnetic resonance ( $^{13}\text{C}$ -NMR) refers to the existence of more than one crystalline form, is called polymorphism (Perez and Samain, 2010), four major polymorphs of cellulose have been reported, cellulose I, II, III and IV (Mandal and Chakrabarty, 2011). The relationships of the different cellulose allomorphs and some prototypical fibers diffractograms showed in Figure 3.

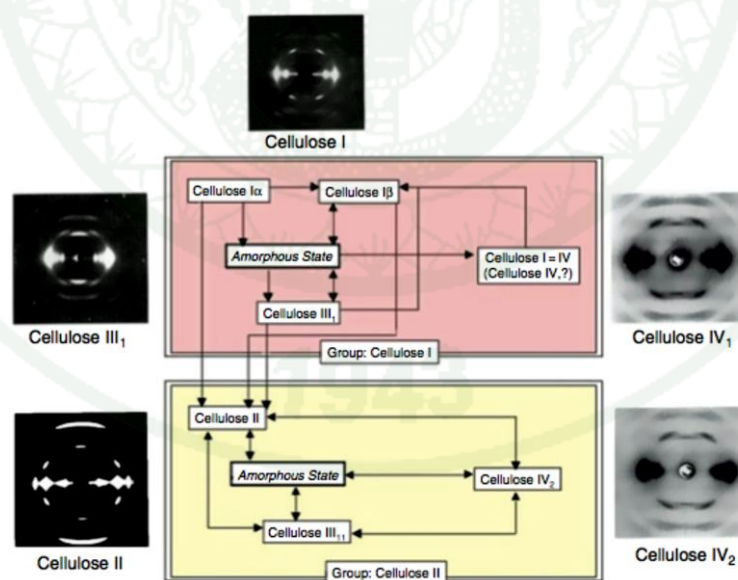


**Figure 3** Relationships of the different cellulose allomorphs and some prototypical fibers diffractograms.

**Source:** Perez and Samain (2010)

Generally, cellulose I is the native cellulose and predominant in nature such as bacteria, some animals and higher plants. Cellulose I or native cellulose can be converted into other polymorphs depending on various of isolation treatments. Moreover, cellulose I has two forms, cellulose I<sub>α</sub> and cellulose I<sub>β</sub>. Cellulose I<sub>α</sub> is predominant in bacteria and algae while cellulose I<sub>β</sub> is predominant in higher plant (Liu and Sun, 2010). On the resulting of <sup>13</sup>C-NMR spectra of cellulose I that shown different at ~106 ppm, I<sub>α</sub> is singlet while I<sub>β</sub> is doublet, the conformation of the polysaccharides is similar although the hydrogen bonding is different (Siqueira *et al.*, 2010). Cellulose III is obtained from in both cellulose I and II, which treated with liquid ammonia at -80 °C. Cellulose IV is obtained by heating either cellulose III in glycerol at 260 °C, its generated cellulose IV, depending on the starting material (Perez and Samain, 2010).

### **Nanocellulose fibers**

Over 30 years, cellulose fibers have been applied in many applications, such as paper and pulp industries, membrane, fibers, composites, cosmetic, drug delivery and medical implant as well (Klemm *et al.*, 2005). Because of cellulose have potential properties, such as high mechanical properties, high thermal stability as well as high water holding capacity. Moreover, cellulose have been studied by numerous researchers in order to improve cellulose properties and their composites and to create a new properties and functions (Brinchi *et al.*, 2013). Recently, the cellulose in nano-dimensional structure, namely nanocellulose, has been growing interested for many researches because of its displays unique characteristics, such as very large surface to volume ratio, high surface area, good mechanical properties including high Young's modulus, high tensile strength, high elasticity (Chen *et al.*, 2011; Klemm *et al.*, 2011), and low coefficient of thermal expansion (Kaushik *et al.*, 2010). In case of the morphology of cellulose nanofibers is nano-whisker or rod-like shape. Commonly, diameter and length of nanocellulose present ranging 5-15 nm and 100-300 nm, respectively (Klemm *et al.*, 2005), which depended on extraction methods, chemical agents use, reaction time, temperature (Rosa *et al.*, 2010) as well as cellulose sources. At same time, the applications of nanocellulose have been extending interested for

research involves the use of nanocellulose in many fields for stance of nanocellulose filler or reinforcing agents in many polymers to improve their properties.

The size, shape, functions, properties of nanocellulose depend mainly on the cellulosic source and preparation methods used (Brinchi *et al.*, 2013). Klemm *et al.* (2011) and Brinchi *et al.* (2013) proposed about the nomenclature of nanocellulose in many types, as indicated in Table 2. Over the past several decades, the challenges in production of nanocellulose, several studies have been used the plant-based cellulose as source to generate nanocellulose using different techniques. The schematic of the tree hierarchical structure to single cellulose chain reveal in Figure 4.

**Table 2** Type of nanocellulose.

Type	Synonyms	Typical source	Average size
Nanocrystalline cellulose	Cellulose nanocrystals, crystallites, whiskers,	Wood, cotton, hemp, flax, straw, mulberry bark, ramie, MCC, bacteria	Diameter: 5–70 nm Length: 100–250 nm (from plant)
Microfibrillated cellulose	Microfibrillated cellulose, nanofibrils, microfibrils, nanofibrillated cellulose	Wood, sugar beet, potato tuber, hemp, flax	Diameter: 5–60 nm Length: several $\mu\text{m}$

**Source:** Brinchi *et al.* (2013)

Recently, the research is focusing on the possible use of forest or agricultural residues as cellulose source for preparing nanocellulose due to their abundance in nature, low cost and energetic cost as well as for the simplified waste disposal (Brinchi *et al.*, 2013). Therefore, there are many researches have been used many source for attempts of nanocellulose preparation using different techniques. For

example nanocellulose has been isolated from lignocellulosic materials, especially, agricultural waste residues, summarized in Table 3.

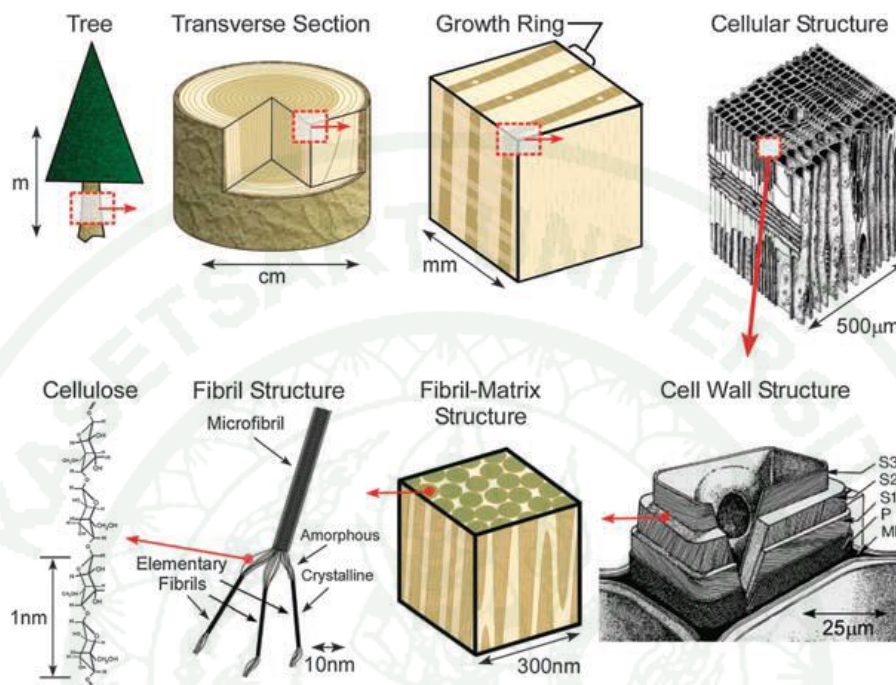


**Figure 4** Schematic of the tree hierarchical structure.

**Source:** Moon *et al.* (2011)

**Table 3** Various natural fibers for isolation of nanocellulose.

Sources	References
Banana rachis	Zuluaga <i>et al.</i> , 2008; Deepa <i>et al.</i> , 2011
Cotton	Teixeira <i>et al.</i> , 2010
Coconut husk	Rosa <i>et al.</i> , 2010
Curana fibers	Corrêa <i>et al.</i> , 2009
Pea hull fibre	Chen <i>et al.</i> , 2009
Pineapple leaf	Cherian <i>et al.</i> , 2010
Sisal	Moran <i>et al.</i> , 2008
Sugarcane bagasse	Mandal <i>et al.</i> , 2011
Wheat straw, soy hulls	Alemdar and Sain, 2008

### Preparation of nanocellulose

The concepts of nanocellulose preparation involves about the difference of cellulose structure. It is well known that cellulose structure has two major regions (Figure 5). One is crystalline regions (some authors called ordered structure) and one is amorphous regions. Resulting from those regions has different properties such as thermal properties and digestibility. Thus, the amorphous regions can destroy by different treatments before crystalline region because of the treatment process starts with the cleavage and destruction of the more readily accessible amorphous regions to liberate rod-like crystalline cellulose sections. Therefore, several researches have been studied attempt to eliminate amorphous region using different techniques in order to generate crystalline nanocellulose fibers. After remove the amorphous region, the residue crystalline region of cellulose chain exhibited the rod-like shape in nano-dimensional structure, depending on source and methods used, which present the potential properties such as high crystallinity, good mechanical properties, high aspect ratio when compared with native cellulose.

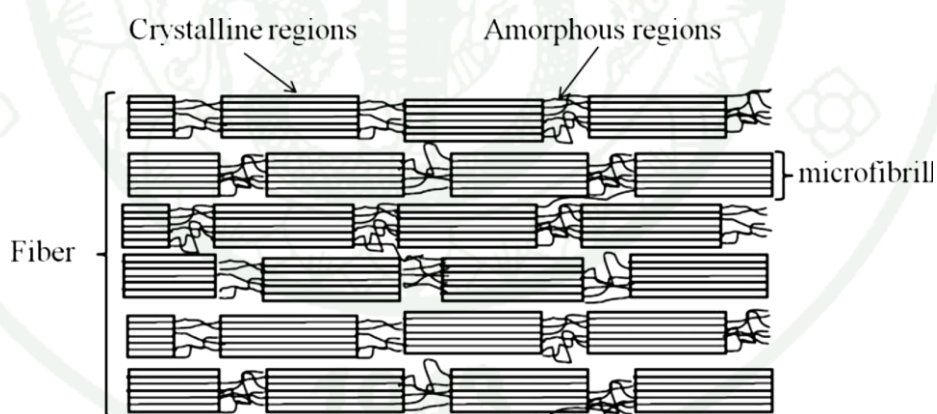


**Figure 5** Schematic diagram of the physical structure of a semi-crystalline cellulose fibers.

**Source:** Spence *et al.* (2011)

Briefly, nanocellulose preparation from lignocellulosic materials divides to two stages. The first one is extraction of cellulose from cellulose source materials (as described in cellulose extraction). The second one is a controlled preparation methods to remove the amorphous regions of the cellulose chain (Brinchi *et al.*, 2013). Scheme of main steps needed to prepare nanocellulose from lignocellulosic biomass shown as Figure 6.

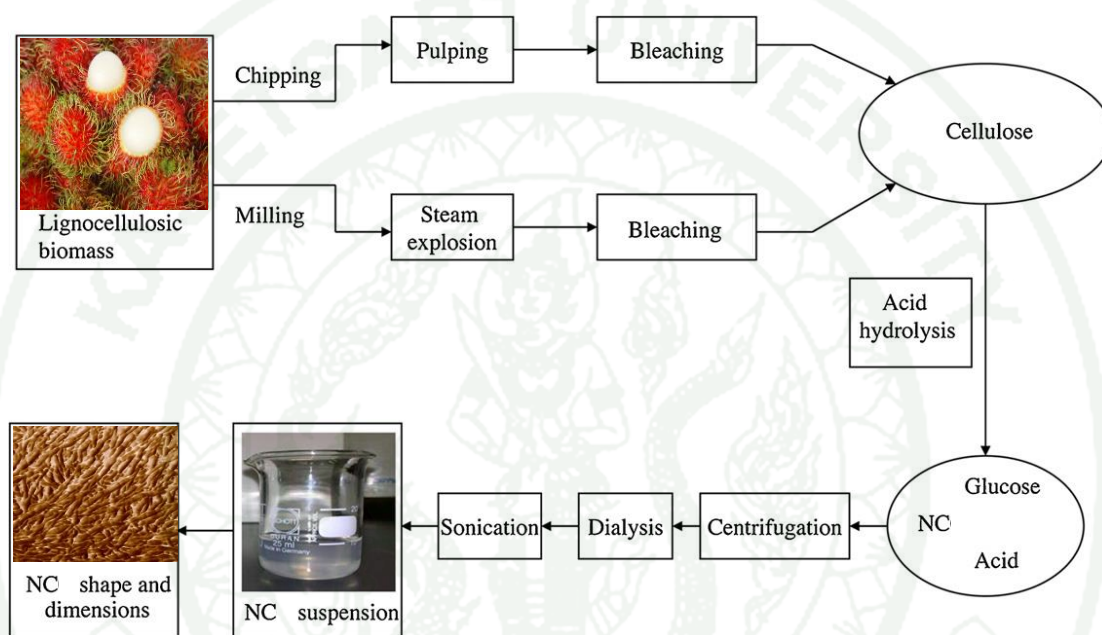


**Figure 6** Scheme of main steps needed to prepare nanocellulose from lignocellulosic biomass (NC = nanocellulose).

**Source:** Adapted from Brinchi *et al.* (2013)

## 1. Cellulose extraction

Plant-based cellulose has been extracted from a variety of lignocellulosic materials which is well-known that consists of complex structure. The cellulose in plant cell wall is embedded to amorphous non-cellulosic materials including, lignin, hemicellulose, and other polysaccharides (Abraham *et al.*, 2011). Hence it is necessary to eliminate non-cellulosic materials using chemical or physico-chemical treatments upon cellulose source. The different approaches have been applied to

isolated cellulose from different materials, depending on the cellulose sources and processes used (Klemm *et al.*, 2005; Lu and Hsieh, 2010; Klemm *et al.*, 2011). Several processes have been used to extract highly purified nanocellulose from cellulosic materials (Table 3). All these methods lead to different types of nanofibrillar materials, depending on the cellulose raw material and its pretreatment (Chen *et al.*, 2009; Mandal and Chakrabarty, 2011; Khalil *et al.*, 2012).

Traditional methods of cellulose extraction based on the use of many chemical solvents, which used to remove the non-cellulosic materials such as lignin, hemicellulose and other polysaccharides. For instance chemical extraction methods, alkaline extraction, alkaline peroxide extraction, lime extraction, organic solvent extraction and acid hydrolysis (Mosier *et al.*, 2005; Liu and Sun, 2010). The chemical extraction is effective method to extract cellulose due to low cost and easy to control, however, these methods also generate the chemical wastes that effect on environment, resulting in the growing research about the use of environmental friendly methods for reduce or replace the chemical extraction.

### 1.1 Pretreatment by steam explosion

Steam explosion is main methods developed recently to isolate cellulose from hardwood and agricultural waste residues, especially for the production of bioethanol (Abraham *et al.*, 2013). Recently, this method has been used in the modification of cellulosic fibers such as flax, banana fibers (pseudo stem), and pineapple leaf. The advantages of steam explosion include a significantly lower environmental impact, lower energy consumption, lower capital investment, and less hazardous process chemicals, compared with chemical treatments (Mosier *et al.*, 2005; Cherian *et al.*, 2008).

Steam explosion is to be subsequently used in chemical fractionation, biotechnological conversion, and the production of panels and composites (Cherian *et al.*, 2008). High pressure steaming followed by rapid process included saturating the dry materials with steam at elevated pressure and temperature followed by sudden release of pressure during which the flash evaporation of water exerts a thermo

mechanical force causing the material to rupture. Indeed, the steam explosion process has been divided into two phases, namely, steam treatment at an elevated temperature and the subsequent explosive defibration (Cherian *et al.*, 2008; Deepa *et al.*, 2011). The steam explosion process results in the hydrolysis of glycosidic bonds in hemicellulose and to a lesser extent in cellulose. It also leads to a cleavage of hemicellulose-lignin bonds. The reactions result in an increased water solubilization of hemicelluloses and in an increased solubility in alkaline or organic solvents, leaving the cellulose as a solid residue with a reduced degree of polymerization (DP) (Cherian *et al.*, 2008). Several authors reported the steam explosion can significantly remove the hemicelluloses in lignocellulosic materials due to the partially hydrolyzed during steam explosion and some lignin are depolymerized, resulting in sugars and phenolic compounds that are soluble in water (Liu and Sun, 2010). Mosier *et al.* (2005) proposed about steam explosion mechanism, steam provides an effective vehicle to rapidly heat cellulosic to the target temperature without excessive dilution of the resulting sugars. Rapid pressure release rapidly reduces the temperature and quenches the reaction at the end of the pretreatment. The rapid thermal expansion used to terminate the reaction opens up the particulate structure of the biomass but enhancement of digestibility of the cellulose in the pretreated solid is only weakly correlated with this physical effect (Deepa *et al.*, 2011; Abraham *et al.*, 2013). The schematic presentation of physical effects of pretreatment on lignocellulosic biomass shows in Figure 7.

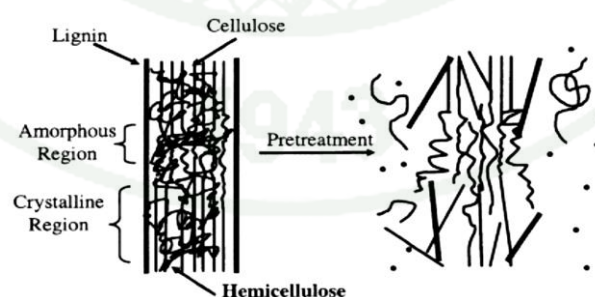


**Figure 7** Schematic presentation of effects of pretreatment on lignocellulosic biomass.

**Source:** Mosier *et al.* (2005)

Cherian *et al.* (2008) reported the steam explosion, alkaline solution (bleaching) followed by acid treatment to produce the cellulose nanofibril from banana fibers (pseudo stem of the banana plant *Musa sapientum*). The steam explosion followed by acidic medium (oxalic acid) is found to be effective in the depolymerization and defibrillation of the fibers to produce banana nanofibers. The chemical compositions of untreated, steam-exploded, bleached banana fibers were determined. The percentage of cellulose contents were found to be increased during steam explosion and the additional bleaching process, while the lignin and hemicellulose content decreased from untreated to bleached fibers.

## 1.2 Bleaching

A protocol based on acidified chlorite solution is mostly applied to delignify lignocellulosic materials in the isolation of cellulose and sodium hydroxide (NaOH) under high temperature (70-80 °C) also widely used as initial steps. These solvents are effectively method, which used for eliminate almost all of hemicellulose and lignin from several biomass (Corrêa *et al.*, 2010). In addition, the use of sodium chlorite called alkaline extraction or bleaching. The chemical extraction is effective method to extract cellulose due to low cost and easy to control, however, these methods also generate the chemical wastes that effect on environment, resulting in the growing research about the use of environmental friendly methods for reduce or replace the chemical extraction.

The immersion of lignocellulosic fibers in dilute alkaline medium facilitates the adhesive nature of the fibers surface by removing natural and other impurities and causes the separation of structural linkages between lignin and carbohydrate and the disruption of lignin structure. The aim behind the bleaching process is the removal of lignin left after the alkaline steam treatments. The bleaching treatment done in the presence of chlorite solution popularly used in laboratories to remove lignin from the vegetable fibers helps in the removal of phenolic compounds or molecules having chromophore groups in order to whiten the fibers (Cherian *et al.*, 2008).

## 2. Acid hydrolysis

Several processes have been used to extract highly purified nanocellulose from cellulosic materials. All these methods lead to different type of nanofibrillar materials, depending on the cellulose raw materials and its pretreatment, and more importantly, depending on the disintegration process itself (Khalil *et al.*, 2012). In addition, the preparation processing of nanocellulose in some literatures summarized in Table 4.

The acid hydrolysis is the most well-known and widely used for the preparation of nanocellulose (Bondeson and Oksman, 2007; Chen *et al.*, 2011; Hashaikeh and Abushammala, 2011). For example of chemical agents using for acid hydrolysis, such as sulfuric acid (Mandal and Chakrabarty, 2011), hydrochloric acid (Kaushik and Singh, 2011), oxalic acid (Cherian *et al.*, 2008; Deepa *et al.*, 2011) as well as acid mixture (Corrêa *et al.*, 2010). Generally, acid hydrolysis was carried out with sulfuric acid with constant stirring. The suspension was immediately diluted 10-fold with deionized water to quench the reaction. The suspensions were centrifuged at 10,000-13,000 rpm for 10-30 min to concentrate the cellulose and to remove excess aqueous acid. The resultant precipitate should be rinsed, re-centrifuged, and dialyzed against water for 5 days until constant neutral pH (Khalil *et al.*, 2012). The amorphous regions around the cellulose microfibrils could be destroyed by acid hydrolysis under controlled conditions, keeping the crystallites intact. The acid hydrolysis is selective in cellulose fibrils, resulting in colloid suspensions of cellulose nanofibers (Alemdar and Sain, 2008). Nanocellulose obtained by acid hydrolysis of cellulose chain (microfiber) has a wide range in size, depending on sources and process used. Treating the cellulose fibers (lignin and hemicellulose free) with sulfuric acid involves esterification of hydroxyl groups, besides the hydrolysis of the glycosidic linkages rendering extensive reduction in degree of polymerization (DP) and particle size consequently (Mandal and Chakrabarty, 2011). In order to possible mechanism of interaction between sulfuric acid hydrolysis and cellulose microfibrils involves the rapid protonation of glucosidic oxygen (path (1)) or cyclic oxygen (path (2)) by protons from the acid, followed by a slow splitting of glucosidic bonds induced by the addition of water (Figure 8a). This hydrolysis process yields two fragments with shorter chains while preserving the basic backbone structure. In native

cellulose, it is well known that the cellulose has two major regions. One is amorphous region and one is crystalline region. The amorphous regions are more accessible to acidic molecules and susceptible to the hydrolytic actions than the crystalline region (Lu and Hsieh, 2010). Under controlled hydrolysis, amorphous regions are hydrolyzed before crystalline region which very fast, the most of these regions were eliminated leaving cellulose chain, remaining the crystalline regions in reaction solution. In addition, Figure 8b showed the mechanism of sulfonation during sulfuric acid hydrolysis. The sulfonation of the hydroxyl groups in cellulose structure, which generally proceeds to “cellulose sulfate” (Lu and Hsieh, 2010). The sulfate group in cellulose chain results in the negatively charged surface. Because of the negatively charged, the nanocellulose suspension was shown to be very efficient in preventing the aggregation of nanocellulose driven by hydrogen bonding (Corrêa *et al.*, 2010; Lu and Hsieh, 2010). Moreover, the presence of sulfate groups also effect on the properties of nanocellulose, as described in the next section.

Corrêa *et al.* (2010) studied to prepare cellulose nanofibers obtained from curaua fibers under different conditions including alkali pre-treatment (NaOH 5 wt% and 17.5 wt% solution) and acid hydrolysis ( $\text{H}_2\text{SO}_4$ , HCl and mixture of  $\text{H}_2\text{SO}_4/\text{HCl}$ ). The results showed that all curaua nanofibers presented a rod-like shape and have average diameter and length of 6-10 nm and 80-170 nm, respectively. The mercerization step, NaOH solutions have influenced the crystallinity index and thermal stability of cellulose nanofibers. The NaOH solution 17.5 wt% resulted in more crystalline cellulose nanofibers whereas thermal properties less stable because of the crystalline structure of nanofibers changed from cellulose I to cellulose II. In the case of the effect on the acid type to curaua nanofibers properties were mainly on the degree of polymerization (DP) and thermal stability. HCl solution can introduce aggregation of nanofibers due to the decrease of surface charges. However, it has better thermal stability than sulfuric acid. The use hydrolysis of HCl or a mixture of  $\text{H}_2\text{SO}_4/\text{HCl}$  increases the thermal stability of nanofibers. However, the use of  $\text{H}_2\text{SO}_4$  was highly stable due to sulfate groups on the cellulose surface create a negative electrostatic layer resulting in a more stable in final suspension.

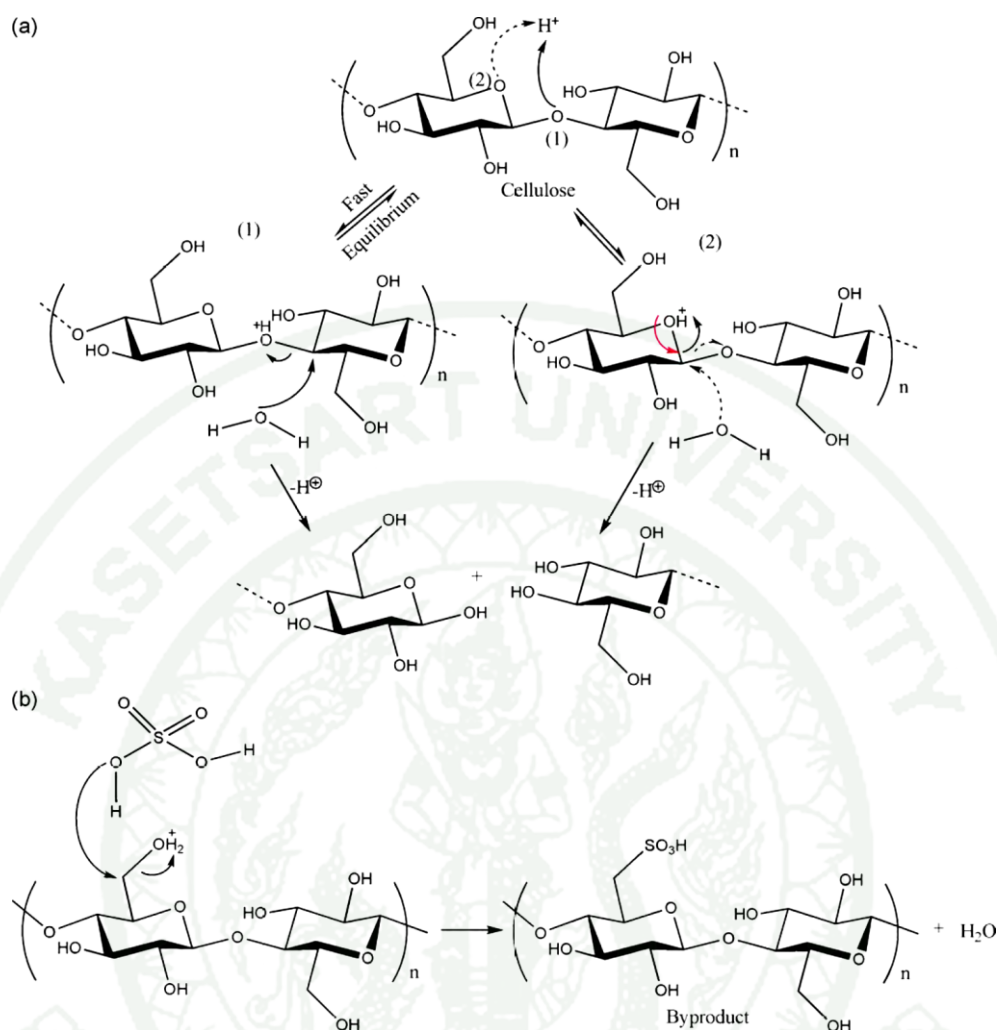


**Figure 8** Acid hydrolysis mechanism (a) and sulfonation of cellulose nanocrystals surfaces (b).

**Source:** Lu and Hsieh (2010)

Mandal and Chakrabarty (2011) has reported the isolation of nanocellulose from sugarcane bagasse (SCB), which is a kind of agricultural waste. Dried bagasse was bleached with 0.7% (w/v)  $NaClO$  at pH 4 and boiled for 5 h to removal hemicellulose. Then, the bleached fibers were boiled with 17.5% (w/v)  $NaOH$  for 5 h to remove the hemicellulose residues. The cellulosic materials were air-dried, and then added to 50 ml dimethylsulfoxide (DMSO) in 80 °C for 3 h. The suspension was subsequently filtered, washed and air-dried. The aqueous suspension of nanocellulose was prepared by acid-hydrolyzed with 60% (w/v) sulfuric acid (fiber to liquor ratio of

1:20) for 50 h at 50 °C under strong agitation. The obtainable nanocellulose has rod-like shape and rods in the nano dimension mostly in the range of 70-90 nm. The thermogravimetric analysis (TGA) of nanocellulose showed that the bagasse starts to degrade earlier than cellulose and the nanocellulose exhibited an even earlier onset of degradation as compared to SCB but leaves the maximum residue within the range of temperature studied. The XRD showed enrichment in the proportion of crystalline cellulose in nanocellulose, which manifests significant conversion of cellulose I to cellulose II. Moreover, this study purpose of DMSO treatment after remove hemicellulose extract cellulose, resulting sulfuric acid can diffuse into fiber more easily, during the acid hydrolysis step.

### 3. Mechanical processes

High-pressure homogenization, grinder/refiners, cryocrushing and high intensity ultrasonic treatments belong to mechanical treatments that used for produce nanocellulose from several cellulose sources. In general these processes produce high shear that causes transverse cleavage along the longitudinal axis of the cellulose microfibrillar structure, resulting in the extraction of long cellulose fibrils (Moon *et al.*, 2011). Several authors reported about the use of mechanical treatments to generate the nanocellulose fibers. However, the nanocellulose obtained from mechanical processes is the particles are generally smaller, more uniform in diameter, but have increased mechanical damage to the crystalline cellulose (e.g. lower percent crystallinity) and these processes require the filtration step to remove the larger unfibrillated and partially fibrillated fractions. In addition, these mechanical processes can be followed by chemical treatments to either remove amorphous material or chemically functionalize the particle surface.

Chen *et al.* (2011) proposed the high-intensity ultra-sonication methods using for prepare nanocellulose from wood (poplar trees). When the output power of ultrasonic treatment used for the chemical-purified cellulose fibers was greater than 1000 W, cellulose nanofibers that are 5–20 nm in width and several microns in length were obtained. Li *et al.* (2012) proposed the nanocellulose isolated from sugarcane bagasse using high pressure homogenization combined with ionic liquid, was found to

be the diameter of nanocellulose is 10-20 nm. Kaushik and Singh (2011) also used the high pressure homogenization to generate nanocellulose from wheat straw. In the case of the ultrasonic technique as method to prepare cellulose nanofibers have been sufficiently described. The ultrasound energy is transferred to cellulose chains. After that, the hydrogen bonds within cellulose chains are destroyed, resulting micro-sized cellulose fibers changed into cellulose nanofibers. However, because of the complicated multilayered structure of plant fibers and the interfibrillar hydrogen bonds, the fibers obtained by ultrasonic methods are aggregated nanofibers with a wide distribution in width (Chen *et al.*, 2009; Wong *et al.*, 2009).

Moreover, the electro-spinning is one of preparation method to generate nanocellulose, which obtained by solutions of cellulose in some solvents (cellulose dissolved in cellulose solvents). It is possible to produce nanofibers of 50-500 nm in diameter, with a high specific surface area and small pore size (Corrêa *et al.*, 2010; Khalil *et al.*, 2012).

**Table 4** Various processes used for isolation of nanocellulose.

Sources	Processes
Sugarcane bagasse (SCB) (Mandal and Chakrabarty, 2011)	1). 0.7% NaCl (pH4), 5 h 2). 5% Na <sub>2</sub> SO <sub>4</sub> , 5 h 3). 17.5% NaOH, 5 h 4). dimethyl sulfoxide (DMSO), 80 °C, 5 h 5). 60% (w/v) H <sub>2</sub> SO <sub>4</sub> , 50 °C, 5 h
Banana fibers (Deepa <i>et al.</i> , 2011)	1). 10% NaOH in autoclave, 6 h 2). NaOH + CH <sub>3</sub> COOH + NaClO, 1h (repeated six times) 3). 11% oxalic acid in autoclave, 3 h
Cotton fibers (Teixeira <i>et al.</i> , 2010)	1). ethanol:cyclohexane (1:1), 12 h 2). 6.5 M H <sub>2</sub> SO <sub>4</sub> , 45 °C, 75 min

**Table 4** (Continued)

Sources	Processes
Wood (poplar tree) (Chen <i>et al.</i> , 2011)	1). 75% NaCl (pH4), 1 h (repeated 5 times) 2). 3% KOH, 80 °C, 2 h 3). 6% KOH, 80 °C, 2 h 4). Ultrasonication (20 kHz, 30 min)
Coconut husk (Rosa <i>et al.</i> , 2010)	1). 2% NaOH, 80 °C, 2 h 2). NaClO <sub>2</sub> (pH4), 1 h (repeated 4 times) 3). 0.05 N HNO <sub>3</sub> , 70 °C, 1 h 4). 64% H <sub>2</sub> SO <sub>4</sub> , 45 °C, 150 min
Sisal fibers (Morán <i>et al.</i> , 2008)	1). 0.7% NaClO <sub>2</sub> (pH4), 2 h 2). 5% Na <sub>2</sub> SO <sub>4</sub> 3). 17.5% NaOH
Soy hulls (Alemdar and Sain, 2008)	1). 17.5% NaOH, 2 h 2). 1 M HCl, 80 C, 2 h 3). 2% NaOH, 2 h 4). Cramer disintergrator (2000 rpm) 5). Homogenization (20 passes, 5 min)
Pineapple leaf (Cherian <i>et al.</i> , 2010)	1). 10% NaOH in autoclave, 1 h 2). NaOH + CH <sub>3</sub> COOH + NaClO, 1h (repeated 6 times) 3). 11% oxalic acid in autoclave, 3 h 4). Mechanical stirrer (8000 rpm), 4 h
Mulberry (Li <i>et al.</i> , 2009)	1). 1% NaOH + 1% Na <sub>2</sub> S, 130 °C, 90 min 2). 0.7% NaOH, 80 °C, 90 min 3). 64% H <sub>2</sub> SO <sub>4</sub> , 60 °C, 30 min
Rice straw (Lu and Hsieh, 2012)	1). Toluene: ethanol (2:1), 20 h 2). 1.4% NaClO <sub>2</sub> (pH4), 70 °C, 5 h 3). 64% H <sub>2</sub> SO <sub>4</sub> , 45 °C, 45 min

## Applications of nanocellulose

### 1. Reinforcing agents

Nanocomposites materials have been widely studied for about the past 20 years. It is a new generation of nanostructure hybrid materials, constitutes a new class of materials, namely nanocomposites. Polymer nanocomposites are defined as polymers containing filler with at least one dimension smaller than 100 nm (Siqueira *et al.*, 2010). There are several cellulose sources, such as banana fibers, cotton, flax, hemp, jute, and sisal and wood fibers, are used to reinforce many composites due to their relative high-strength, high stiffness and low density (Cherian *et al.*, 2011). Many researchers have therefore explored the concept of fully bio-derived nanocomposites as method to development of bioplastics with better properties (Khalil *et al.*, 2012). The use of nanocellulose as reinforcing filler in many polymers matrix is a relatively new area of interest. This is due to the low cost of raw materials and cellulose has numerous found in the nature. Hence, many researchers have been studied the use of nanocellulose reinforced other polymers especially, biopolymers, such as poly(lactic acid) (PLA) (Iwatake *et al.*, 2008; Jonoobi *et al.*, 2012), natural rubber (Pasquini *et al.*, 2010; Abraham *et al.*, 2012), thermoplastic starch (TPS) (Teixeira *et al.*, 2009; Kaushik *et al.*, 2010) as well as other synthetic polymers. It is aimed to improve their properties of host-polymers, such as biodegradability, thermal stability, mechanical properties, water sensitivity, and crystallinity as well as barrier properties.

Iwatake *et al.* (2008) has studied the reinforcement of PLA using cellulose nanofibers. This study was carried out to know the potential of reinforcement by cellulose nanofibers in PLA matrix, with the goal of making sustainable green composites. Cellulose nanofibers have been premixed with PLA using organic solvent, and then the mixture was needed to attain uniform dispersion of cellulose nanofibers. As the results, cellulose nanofibers can increase Young's modulus and tensile strength of PLA by 40% and 25%, respectively, without a reduction of yield strain at a fibers content of 10 % (wt).

In the case of thermoplastic starch (TPS), Teixeira *et al.* (2009) has reported the cassava bagasse cellulose nanofibers reinforced thermoplastic cassava starch. The cellulose nanofibers prepared from cassava bagasse by acid hydrolysis without any purified processes. Adding cellulose nanofibers at 10 wt.% were results in a decrease of the water uptake of thermoplastic starch. This means that the reduction of the hydrophilic nature due to cellulose properties. In addition of glass transition ( $T_g$ ) of the nanocomposites was shifted to higher temperature as compared with to pure TPS.

## 2. Electrical membrane and energy storage

In the past few years, considerable progress has been made in the fabrication of nanocellulose based conducting polymers composites such as polyaniline (PANi) (Luong *et al.*, 2013), polypyrrole (PPy), carbon nanotubes (CNTs) and graphene (Malho *et al.*, 2012), using by several techniques, which can potentially be used as material in many applications such as flexible electrodes, sensors, and electrically conductive films and papers.

Malho *et al.* (2012) prepared the native nanocellulose/graphene (multilayered graphene) nanocomposites to obtain the novel conductive films using by vacuum filtration method. The nanocomposites consisting of aligned assemblies of multilayered graphene and nanocellulose with excellent tensile mechanical properties without any surface treatments. The optimum composition was found at 1.25 wt% graphene, giving a Young's modulus of 16.9 GPa.

Luong *et al.* (2013) studied about polyaniline based nanocellulose composites by situ polymerization technique. Authors reported herein a facile approach for fabrication of highly processable nanocellulose/PANi suspension containing various PANi loading content between 5 to 80 wt.%. The achieved composite paper exhibited high electrical conductivity and good mechanical characteristics.

## MATERIALS AND METHODS

### Materials

#### 1. Equipments

- 1.1 Incubator (Mettler, Germany)
- 1.2 Hot plate stirrer (IKA, Germany)
- 1.3 Overhead stirrer (IKA, Germany)
- 1.4 Water bath (Mettler, Germany)
- 1.5 Balance (Mettler Toledo, Switzerland)
- 1.6 Centrifuge (Sorval Model RC, Germany)
- 1.7 Steam explosion (Nitto Koatsu, Japan)
- 1.8 Sonicator bath (Branson Model 2210R-MT, USA)
- 1.9 Scanning electron microscopy (SEM) (JEOL Model JSM-5600 LV, Japan )
- 1.10 Atomic force microscopy (AFM) (Asylum Model MFD-3D AFM(bio), USA)
- 1.11 Fourier transformed infrared spectrometer (FTIR spectrometer) (Bruker Tensor 27 spectrometer, USA)
- 1.12 X-ray diffraction (XRD) (Philips Model X'Pert Powde, Japan)
- 1.13 Thermogravimetric analysis (TGA) (Mettler Toledo, Model TGA/DSC1, Switzerland)
- 1.14 Beaker (Pyrex, Germany)
- 1.15 Erlenmeyer flask (Pyrex, Germany)
- 1.16 Laboratory bottle duran (Duran, Germany)
- 1.17 Cylinder (Pyrex, Germany)
- 1.18 Dialysis membranes (CelluSeq, USA)

## 2. Chemicals

- 2.1 Acetic acid (CH<sub>3</sub>COOH) (China, Macron)
- 2.2 Hydrogen peroxide (H<sub>2</sub>O<sub>2</sub>) (Australia, Unilab)
- 2.3 Sodium chlorite (NaOCl<sub>2</sub>) (Australia, Univar)
- 2.4 Sodium hydroxide (NaOH) (Australia, Univar)
- 2.5 Sodium hypochlorite (NaOCl) (Thailand, Labscan)
- 2.6 Sulfuric acid (H<sub>2</sub>SO<sub>4</sub>) (Thailand, Labscan)
- 2.7 Distilled water (H<sub>2</sub>O)

## Methods

### 1. Cellulose extraction

The mango and rambutan peels were ground into uniform size of approximately 2-5 cm and washed by distilled water to eliminate the other impurity, then, the peel were dried in hot air oven at 60 °C for 24-48 h. After that, the raw fibers were milled with blender and passed through a 40 mesh screen and then used for the extraction of cellulose.

#### 1.1 Steam explosion

The steam explosion (Nitto Koatsu Co. Ltd, Tsukuba, Japan) were support by Kasetsart Agricultural and Agro-Industrial Product Improvement Institute (KAPI), which located at Kasetsart University as shown in Figure 9. First, the mango and rambutan peels were treated in the steam explosion with a pressure of approximately 1.5 MPa at 200 °C for a period of 4 min. Then, the steam-exploded fibers were removed and subsequently washed in distilled water and dried in oven at 50 °C for 24 h.



**Figure 9** Photographs of steam explosion at Kasetsart Agricultural and Agro-Industrial Product Improvement Institute (KAPI).

## 1.2 Bleaching

The steam-exploded fibers were bleached using a mixture of 5% (v/v) sodium hypochlorite solution. Each bleaching took 1 h under continuous agitation and the process was repeated six times or until fiber become white. After bleaching, the fibers were thoroughly washed in distilled water until the suspension returned to pH neutrality and dried in oven at 50 °C for 24 h (adapted from Deepa *et al.* (2011)).

## 2. Nanocellulose preparation

The bleached fibers were treated with 64% (w/w) H<sub>2</sub>SO<sub>4</sub> at 45 °C for 90 min. A white material in suspension was stop reaction by adding cooled water (4 °C) as anti-solvents. The volume of anti-solvent was equivalent to volume of acid solution used. The cellulose nanofibers were washed with distilled water by centrifugation at 13,000 rpm for 15 min. The precipitate was collected and dialyzed for 3-5 days until pH became 6-7. Then, the fibers were freeze-dried by lyophilization. The overview of nanocellulose production is shown in Figure 10 (adapted from Deepa *et al.* (2011)).

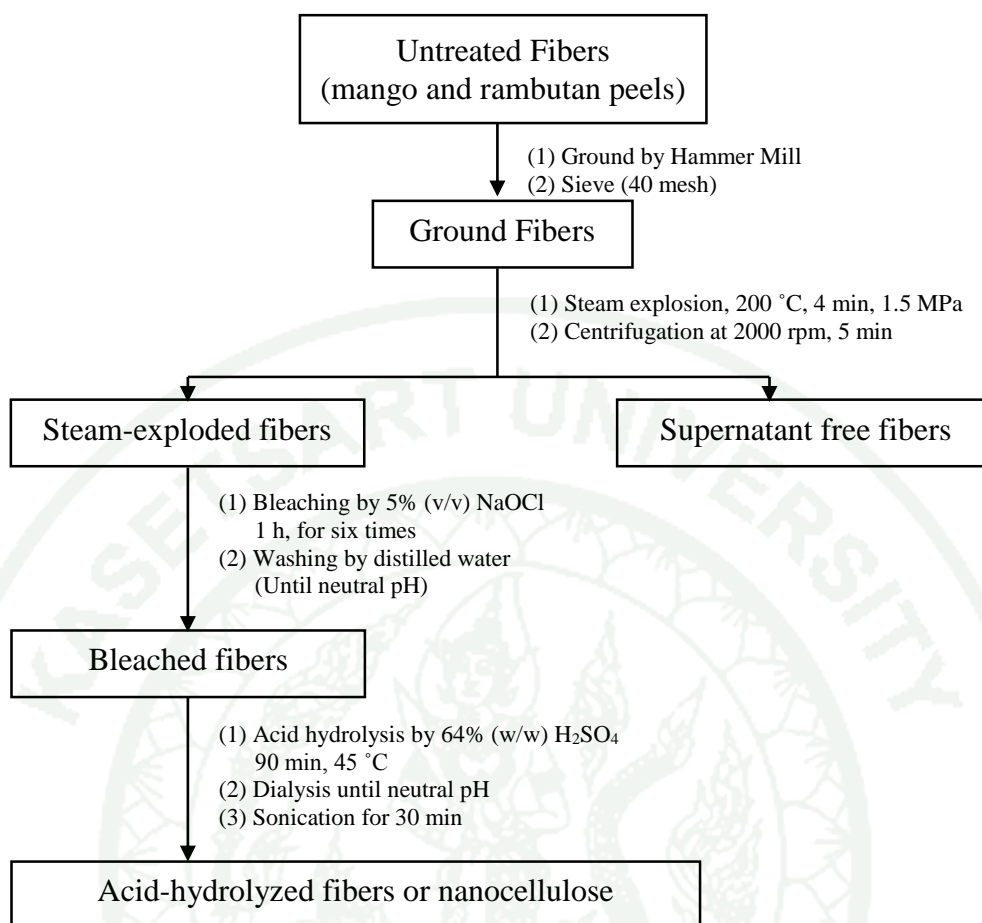


**Figure 10** Scheme for nanocellulose production from mango and rambutan peels.

### 3. Characterization

#### 3.1 Chemical estimation followed by TAPPI standard

The chemical composition of untreated fibers and treated fibers were chemically analyzed for lignin, hemicellulose and cellulose contents. The chemical composition was evaluated following the Technical Association of Pulp and Paper Industry (TAPPI) standard: alpha-cellulose (TAPPI T203 om-88), acid-insoluble lignin (TAPPI T222 om-98) and holocellulose (Acid chlrite's Browing methods).

### 3.2 Scanning electron microscopy (SEM)

Scanning electron microscopy (SEM) (JEOL model JSM-5600 LV (Japan)) was used for structural analysis of untreated fibers and treated fibers. Samples were mounted on a metal stub and gold coat by using sputter coating technique for 20 s to make them conducting. Image of fibers were taken at 20 kV accelerating voltage.

### 3.3 Atomic force microscopy (AFM)

Nanocellulose suspension were observed by atomic force microscopy (tapping mode) using Asylum MFD-3D AFM(Bio) (USA). Calibration was performed by scanning a calibration grid with precisely known dimensions. All scans were performed in the air with commercial tips with a resonance frequency of about 300-330 kHz. Samples of nanocellulose for characterization were prepared by pipetting a 0.01 (w/v) aqueous nanocellulose suspension and allowed to dry on glass slide surface before analysis.

### 3.4 Fourier transform infrared spectroscopy (FTIR)

Fourier transform infrared spectra were recorded using Bruker Tensor 27 spectrometer. Untreated, steam-exploded, bleached and acid hydrolyzed fibers from mango and rambutan peels were analyzed. Samples were finely ground and mixed with potassium bromide (KBr). The mixture was then compressed into pellet form. FTIR spectral analysis was performed within the wavenumber range of 4000-400  $\text{cm}^{-1}$ .

### 3.5 X-ray diffraction (XRD)

X-ray diffraction (Philips, Model X'Pert Powder) equipped with  $\text{CuK}\alpha$  radiation in scattered radiation ranging  $2\theta = 10-40^\circ$  at speed of  $5^\circ/\text{min}$  using for determination of the XRD pattern of the different cellulose samples. The crystallinity

index (Cr.I) was calculated from X-ray diffraction curves by the ratio of the crystalline area to the total area.

$$\text{Cr.I (\%)} = 100 \times (I_{002} - I_{\text{am}}) / I_{002}$$

Where  $I_{200}$  was the maximum intensity of the (0 0 2) lattice diffraction and  $I_{\text{am}}$  was the intensity diffraction at  $2\theta = 18^\circ$  (Segal *et al.*, 1959).

### 3.6 Thermogravimetric analysis (TGA)

TGA (Mettler Toledo, Model TGA/DSC1) utilized to investigation of the thermal stability of different cellulose samples. Sample (~2 mg) was heated from 50 °C to 600 °C at heating rate of 10 °C/min under nitrogen atmosphere with a gas flow of 20 ml/min.

## RESULTS AND DISCUSSION

In this work, mango and rambutan peels were used as cellulose sources. There are two extraction steps which carried out for composed of cellulose extraction from lignocellulosic materials and nanocellulose isolation. Extraction of cellulose was combined between steam explosion and bleaching step, while, acid hydrolysis was exam for nanocellulose production.

### 1. Chemical estimation and its possible mechanism

This work aimed to extract cellulose from mango and rambutan peels using steam explosion combined with bleaching treatment to obtain highly purified cellulose. The chemical compositions of fibers in different processes including untreated fibers, steam-exploded fibers and bleached fibers were determined followed by TAPPI standard in order to estimate the efficiency of extraction processes use. The chemical composition reported as the changes of percentage of  $\alpha$ -cellulose, hemicellulose and lignin during extraction processes.

**Table 5** Chemical composition of mango peel in different treatments.

Materials	Composition (%)		
	$\alpha$ -cellulose	hemicellulose	lignin
Mango peel	38.35 $\pm$ 0.48	13.90 $\pm$ 0.62	27.90 $\pm$ 0.38
Steam-exploded fibers	51.28 $\pm$ 0.24	8.41 $\pm$ 0.05	21.84 $\pm$ 0.61
Bleached fibers	94.21 $\pm$ 0.87	0.42 $\pm$ 0.75	7.42 $\pm$ 0.82

**Table 6** Chemical composition of rambutan peel in different treatments.

Materials	Composition (%)		
	$\alpha$ -cellulose	hemicellulose	lignin
Rambutan peel	54.34 $\pm$ 1.52	7.72 $\pm$ 0.48	36.36 $\pm$ 1.70
Steam-exploded fibers	62.99 $\pm$ 1.05	3.85 $\pm$ 0.31	31.36 $\pm$ 0.40
Bleached fibers	81.26 $\pm$ 0.73	1.87 $\pm$ 0.56	7.72 $\pm$ 0.80

From Table 5, the mango peel raw fibers have the highest percentage of hemicellulose and lignin and lowest percentages of  $\alpha$ -cellulose because it composes of many substances such lignocellulosic materials as well as other polysaccharides. In addition, mango peel has approximately 38 percent of  $\alpha$ -cellulose content, indicating that mango peel is suitable for use as cellulose source. After the steam explosion, the hemicellulose and lignin content were decreased from 13.90% to 8.41% and 27.90% to 21.84%, respectively, while the  $\alpha$ -cellulose content increased from 38.35% to 51.28%. Likewise, rambutan peel revealed the same trend in chemical composition when the rambutan peel subjected to steam explosion, as shown in Table 6. After steam explosion, the hemicellulose and lignin content were decreased from 7.72% to 3.85% while the  $\alpha$ -cellulose content increased from 54.34% to 62.99%, indicating the steam explosion significantly remove of hemicellulose from the rambutan peel. Although, the lignin content in both fibers were slightly decreased because the interaction between lignin and cellulose matrix is relatively strong.

Possibility mechanism of steam explosion involved the hemicellulose is partially hydrolyzed and the depolymerized of lignin (Deepa *et al.*, 2011). The high temperature and high pressure held for a period of time (minutes) as well as the rapid reduction of the pressure during steam explosion significantly eliminate hemicellulose and some lignin by the auto-hydrolysis of hemicellulose fraction and depolymerized of lignin. Mosier *et al.* (2005) proposed the mechanism of steam explosion also involved the hemicellulose is thought to be hydrolyzed by acetic acid and other acids released during steam explosion. The acetic generate from hydrolysis of acetyl groups

associated with the hemicellulose may further catalyze hydrolysis and glucose or xylose degradation, giving rise to sugars and phenolic compounds that are soluble in the water (Cherian *et al.*, 2010; Deepa *et al.*, 2011).

There are many literatures proposed the use of steam explosion with NaOH to generate the steam-exploded cellulose. The NaOH solution occur in steam explosion suggested that there is a partial breakdown of the intermolecular hydrogen bond at the C-3 and C-6 positions of the glucopyranose unit results in significant variations in the network and strength of the hydrogen bonds of the cellulose hydroxyls (Yamashiki *et al.*, 1990; Cherian *et al.*, 2010). However, sodium hydroxide solution was not used in this work, namely uncatalyzed steam explosion. Because this work attempted to reduce the use of chemical agents. Amount of cellulose content in mango and rambutan peels after steam explosion increased approximately 51.28% and 62.99%, respectively, indicating that the steam explosion without NaOH solution was competent process.

However, the removal of non-cellulosic materials is not uncompleted. Therefore, the bleaching step is a potential method which used to eliminate the remaining non-cellulosic substances. The main perspective of bleaching process is the removal of the lignin by oxidation reaction of lignin that leads to lignin dissolution and degradation (Mandal and Chakrabarty, 2011), to obtain the white precipitated, called cellulose. The bleaching by chlorite solution has been attributed to its ability to react with various carbonyl-containing structures in lignin, resulting in the aromatic ring of lignin will be destroyed and converted into carboxylic acid results in soluble in water. This work was used the sodium hypochlorite (NaClO) as bleaching solvent under ambient temperature in order to reduce the energy consumption in bleaching process. The bleaching by NaClO must be used several times for removal of remaining lignin. Figure 11 shows the changes of color of bleaching suspension (fibers:liquor to 1:8).

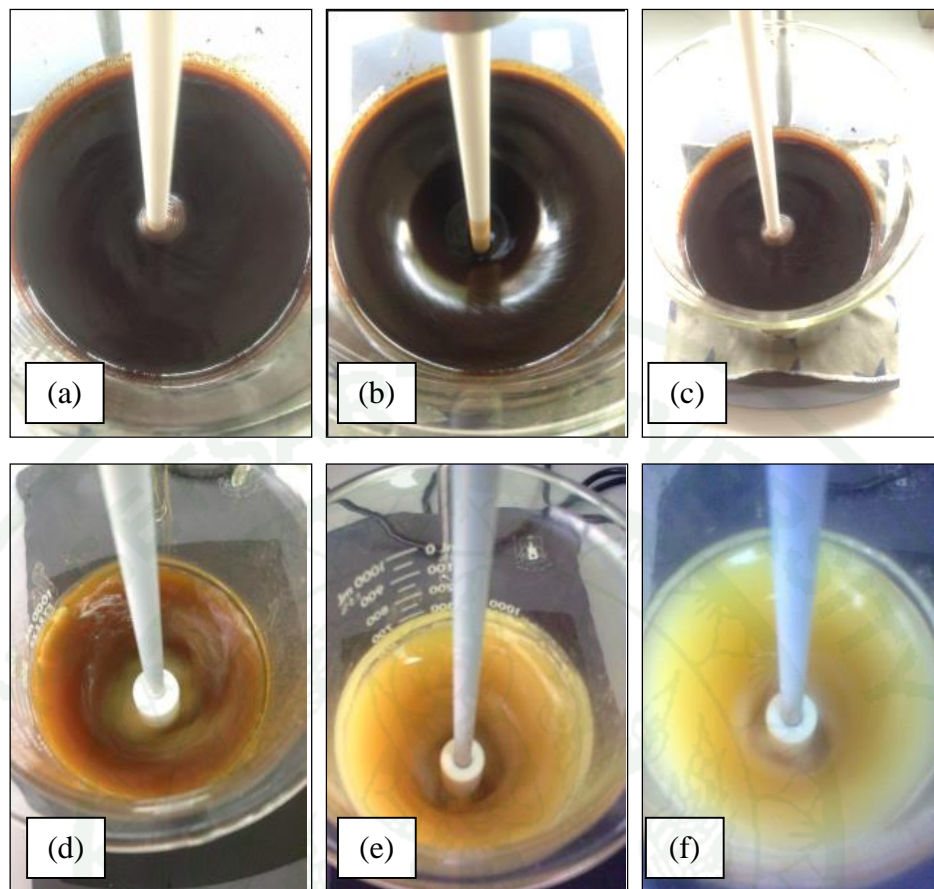


**Figure 11** Bleaching at different processing stages; one times (a), two times (b), three times (c), four times (d), five times (e) and six times (f).

Traditionally, bleaching step has been widely used under high temperature (70-80 °C) to obtain the white cellulose powders (Sun *et al.*, 2004; Morán *et al.*, 2008; Li *et al.*, 2009; Rosa *et al.*, 2010; Mandal and Chakrabarty, 2011). Hence, it is unsuitable in pilot scale because of high temperature requirement, resulting in the high energy consumption. The efficiency of bleaching under ambient temperature is exhibited that lignin content in steam-exploded fibers in mango and rambutan peels were decreased from 21.84% to 7.42% and 31.36% to 7.72%, respectively. On the other hand, the amount of achievable cellulose from mango and rambutan peels after bleaching treatment were 94% and 81%, respectively. It can be concluded that the combination of steam explosion and bleaching treatment are the effective methods for cellulose extraction.

In addition, Figure 12 showed that the photograph of untreated, steam – exploded fibers and bleached fibers. It can be seen that the color of untreated fibers (Figure 12a) showed the brown because it composes of many components. After steam explosion, the color of fibers were changed from brown into brown dark (Figure 12b) because of the browning reaction of other polysaccharides in fibers. When steam-exploded fibers subjected to bleaching process, the color of fibers became white (Figure 12c) due to the removal of lignin and hemicellulose in the components.



**Figure 12** Photographs of mango peel; untreated fibers (a), steam-exploded fibers (b) and bleached fibers (c).

## 2. Morphology analysis

The structural and surface morphologies of the untreated fibers, steam-exploded fibers and bleached fibers were obtained by scanning electron microscope (SEM) analysis and the SEM micrographs of mango and rambutan peels are shown in Figure 13 and Figure 14, respectively.

Figure 13a showed that the SEM photograph of untreated mango fibers revealed the complex structure with certain of plant cell wall structure. When the fibers subjected to steam explosion, the surface morphology of fibers also changed during this treatment, which monitoring by SEM microscopy. Figure 13b the surface morphology observed in micro-scale of steam-exploded fibers in order to study about the physical effects of steam explosion on the morphological property. In this work was collected the SEM image of untreated and steam explosion fibers at the same magnification (x500) to compare the changes of surface morphology of fibers after treated with steam explosion. In mango peel, the difference of the SEM micrographs between untreated fibers and steam-exploded fibers are shown in Figure 13a and 13b respectively, it is clearly that the surface of steam-exploded fibers exhibited rough surface result from the disruption of cell wall. In case of the disruption of fibers structure due to the rapidly reduction of pressure during steam explosion which hold in high pressure, resulting the water in the fibers is exploded to atmospheric pressure (Sun and Cheng, 2002). In the case of rambutan peel, the morphology of untreated fibers obtained from SEM microscopy shown in the Figure 14, which revealed the complex structure which appears smooth surface because of it has waxes and oil in the components. After steam explosion, the fibers present a rough surface when compared with the untreated fibers at the same magnification (x2000). This is due to the partial hydrolysis of hemicelluloses and defibrillation of lignin, resulting in these substances will be soluble in water. As well, the SEM image of steam-exploded fibers from rambutan peel (Figure 14b) shows the rough surface due to eliminate of hemicellulose, lignin some loose substance from the surface of fibers.

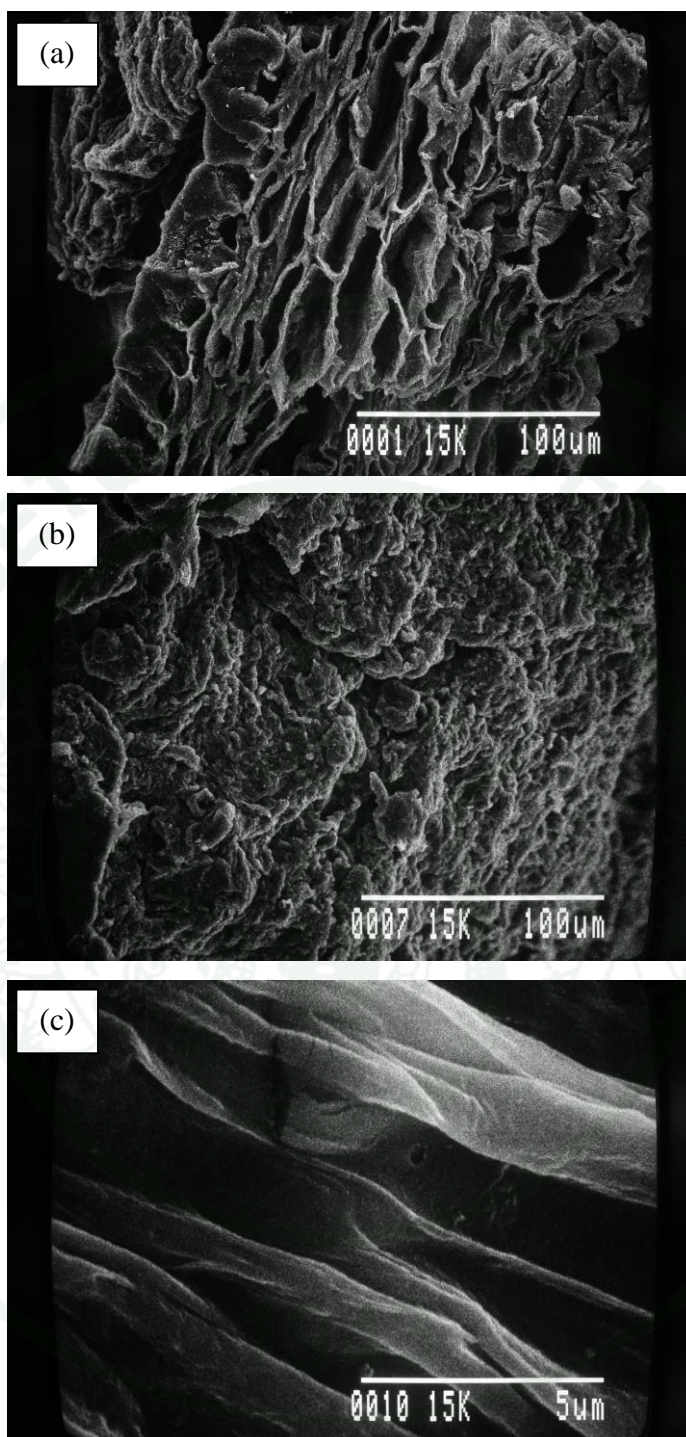


**Figure 13** Scanning electron micrograph of mango peel; untreated fibers (a), steam-exploded fibers (b) and bleached fibers (c).

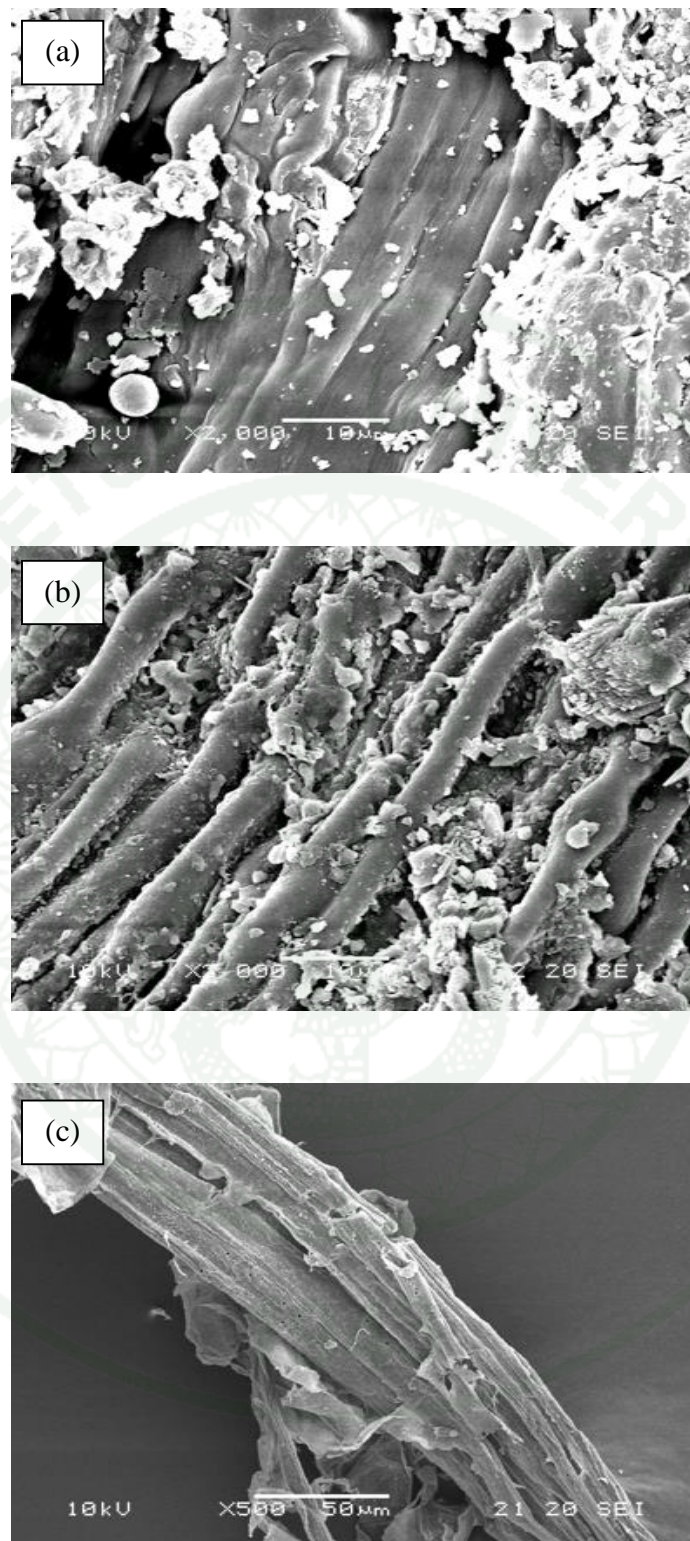


**Figure 14** Scanning electron micrograph of rambutan peel; untreated fibers (a), steam-exploded fibers (b) and bleached fibers (c).

Regarding to chemical composition of steam-exploded fibers in raw materials, the residue of lignin content was still high which indicated that the steam explosion could not completely remove lignin and other substances. Hence, bleaching by sodium hypochlorite is needed for removal of remaining of non-cellulose substances. The SEM image of bleached mango fibers (Figure 13c) showed the diameter of fibers around 1-3  $\mu\text{m}$ . These fibers exhibited the smooth surface, that it could be the completely removal of non-cellulosic materials. However, some authors proposed that bleached fibers exhibited rough surface during extraction because the removal of the wax and oil as well as other polysaccharides. On the other hand, SEM photograph of the bleached fibers (Figure 14c) from rambutan peel presented the rough surface than untreated fibers due to the elimination of non-cellulosic materials. It can be seen that bleached fibers showed the microfibrils bundle of cellulose fibril and the diameter of the microfibrils average of 50  $\mu\text{m}$ .

### **3. Morphology of nanocellulose and its possible acid hydrolysis mechanism**

There are several researches studied about the preparation of nanocellulose from lignocellulosic materials, especially, plant based cellulose. Several investigations have been studied and optimized condition of nanocellulose extraction from cellulose. In plant cellulose, the acid hydrolysis is the most widely used with 64% (w/w) sulfuric acid for 45-90 min (Lu and Hsieh, 2010; Rosa *et al.*, 2010; Klemm *et al.*, 2011). Diameter and size of nanocellulose are depends on preparation condition and cellulose sources. Therefore, this work used sulfuric acid hydrolysis under 45 °C for a period of 90 min to generate nanocellulose from bleached fibers. Generally, microscopy has been the preferred technique for studied the morphological characteristic of nanocellulose. In this study, atomic force microscope (AFM) was used to investigate the morphology, size and shape because of AFM technique was used to observe in nano-scale (above 1 nm). The AFM topographies of nanocellulose from mango and rambutan peels showed in Figure 15 and 16, respectively.

AFM height images collected under tapping mode displayed typical shape of nanocellulose from mango (Figure 15a) and rambutan peels (Figure 16a) revealed as nano-dimension around 5-40 nm and exhibited numerous and overlapped fibers. In addition, AFM phase images were similar, which exhibit the size and dimension of nanocellulose from mango peel (Figure 15b) and rambutan peel (Figure 16b), having the rod-like shape. This indicates AFM image proves that the acid coupled steam defibrillation leading to individualization of nanocellulose from the cell wall without degrading them.

In addition, the size distribution calculated using the computer program Gwyddion for obtained the height distribution of nanocellulose in both mango peel (Figure 17a) and rambutan peel (Figure 17b). An important consequence of the observed size reduction is the increase in the fiber aspect ratio ( $L/D$ ,  $L$  being the length and  $d$  the diameter), which should provide higher reinforcing capability of the fibers for composite applications (Johar *et al.*, 2012). The diameter distribution of obtainable nanocellulose extracted from both mango and rambutan peels are shown in Figure 17a and Figure 17b, respectively. The most nanocellulose fibers from mango peel displayed a diameter, length and aspect ratio in the range of 10-15 nm, 150-200 nm and 13-15 respectively, whereas the most nanocellulose fibers from rambutan peel exhibited in the range of 5 nm, 150-200 nm and 30-40.

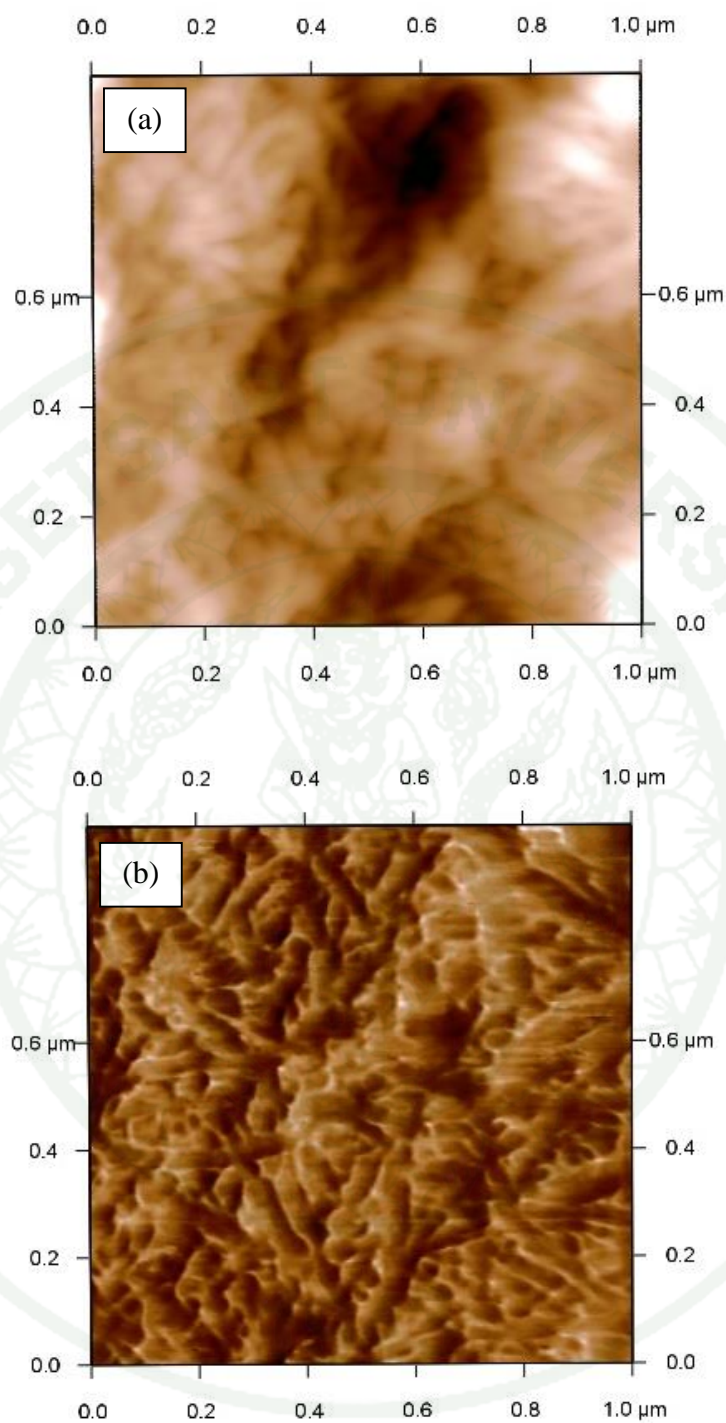


**Figure 15** AFM photograph of nanocellulose from mango peel; height image (a) and phase image (b).

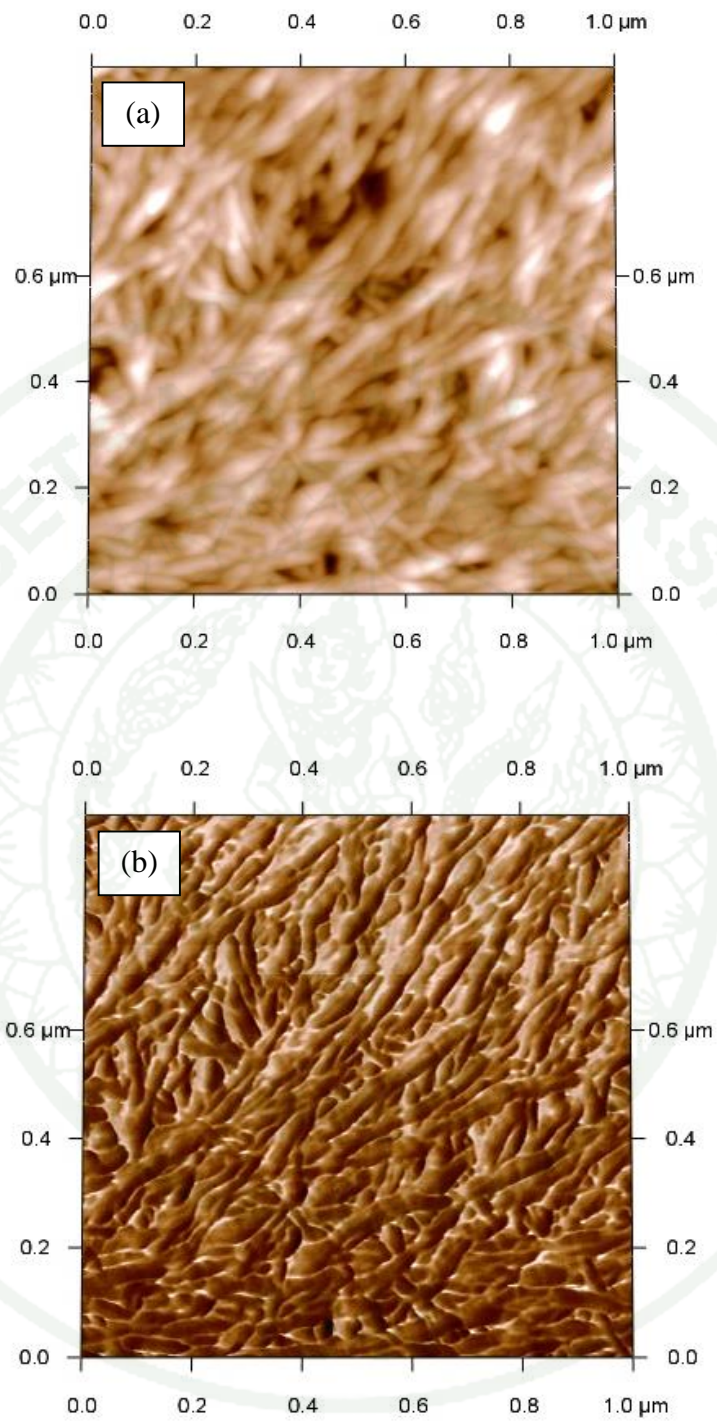


**Figure 16** AFM photographs of nanocellulose from rambutan peel; height image (a) and phase image (b).

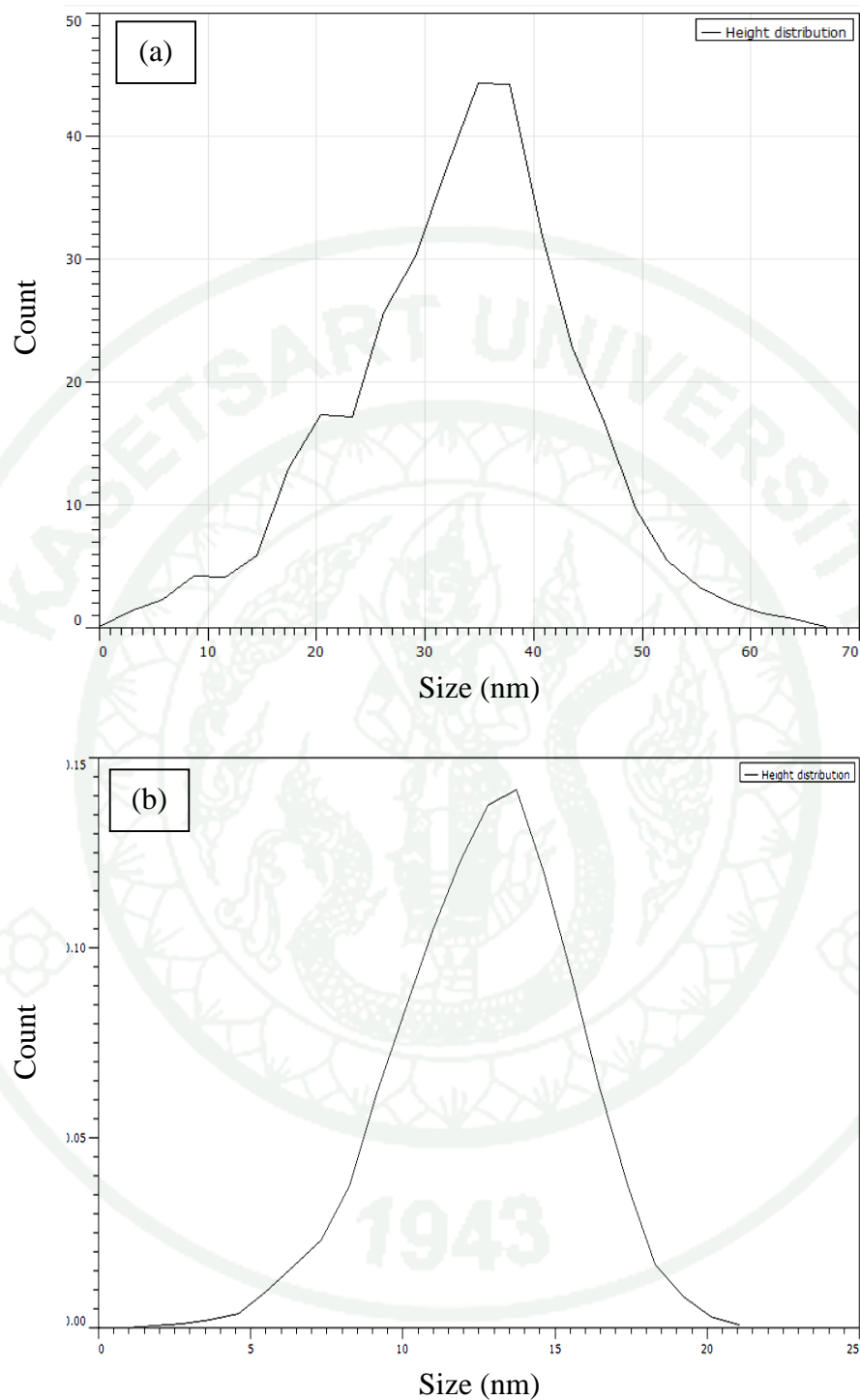


**Figure 17** Height distribution of diluted nanocellulose (0.01 mg/ml) from mango peel (a) and rambutan peel (b) analyzed by Gwyddion program.

#### 4. Functional groups analysis

The changes of fibers structure during isolation processes were monitored by fourier transform infrared (FTIR) spectroscopy which used to confirm the change of chemical composition of fibers during isolation processes. In addition, FTIR determination was used to investigate the effect of physic-chemical on the functional groups of the fibers during cellulose extraction (steam explosion and bleaching) and nanocellulose preparation (acid hydrolysis). FTIR spectrometer simultaneously collects spectral data in a wide spectral range (this work was collected in ranging 4000-400  $\text{cm}^{-1}$ ). Briefly, in infrared spectroscopy, irradiation is passed through a sample. Some of the infrared radiation is absorbed by the sample and some of it passes through. The resulting spectrum represents the molecular absorption and transmission, creating a molecular fingerprint of the sample (a fingerprint no two unique molecular structures produce the same infrared spectrum) (Liu and Sun, 2010).

Figure 18 and 19 showed the FTIR spectra of untreated fibers, steam-exploded fibers, bleached fibers and acid-hydrolyzed fibers of mango and rambutan peels, respectively. In addition, infrared transmittance spectra with main observed peaks of the mango peel fibers and rambutan peel fibers in different stages are shown in Table 7 and Table 8, respectively. In all samples, the FTIR spectra exhibited a broad band near 3400-3300  $\text{cm}^{-1}$  represented that the free OH stretching vibration of the O-H groups, due to the water absorbed in sample (moisture in the samples) (Abraham *et al.*, 2011; Mandal and Chakrabarty, 2011). On the other hand, the increase of the cellulose content during isolation process is evident from the increased intensity of the peak between 3400-3300  $\text{cm}^{-1}$  bands.

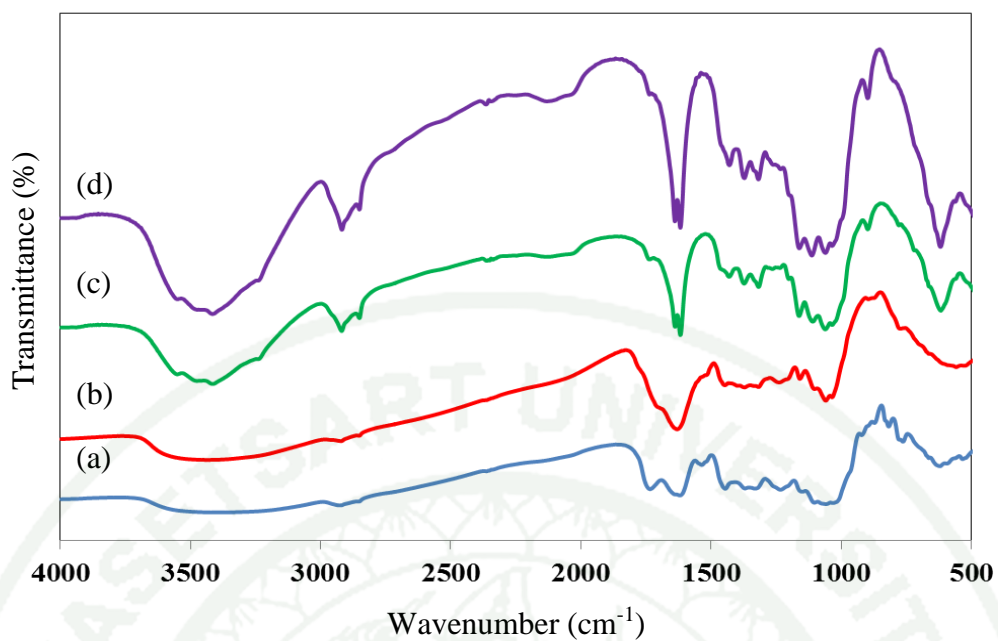


**Figure 18** FTIR spectra of mango peel; untreated fibers (a), steam-exploded fibers (b), bleached fibers (c) and acid-hydrolyzed fibers (d).

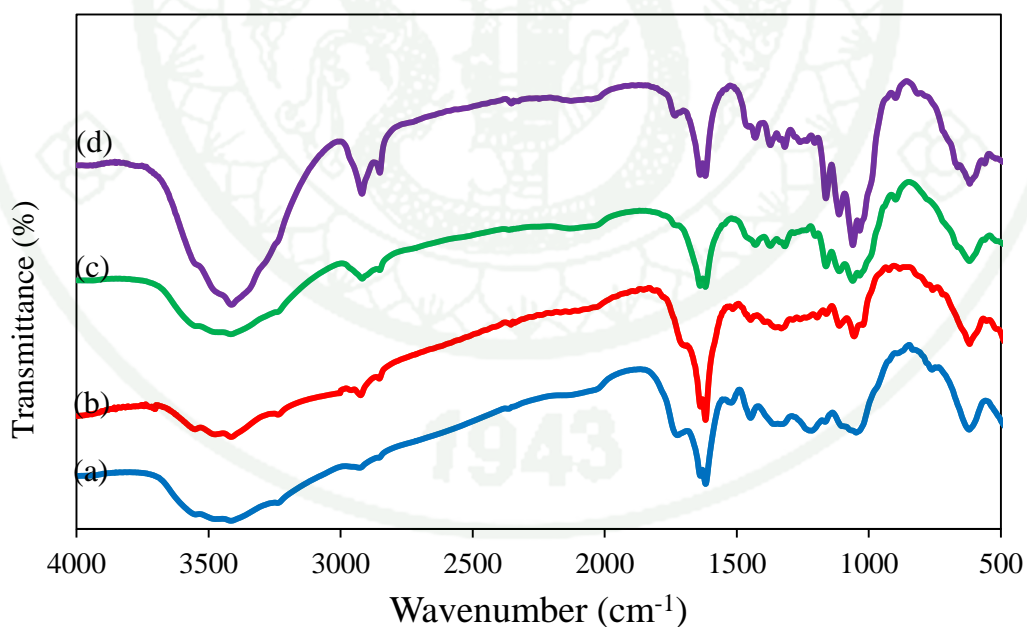


**Figure 19** FTIR spectra of rambutan peel; untreated fibers (a), steam-exploded fibers (b), bleached fibers (c) and acid-hydrolyzed fibers (d).

**Table 7** The dominant peak absorption of mango peel in different fibers.

Functional groups	Absorbance peak (cm <sup>-1</sup> )			
	Untreated fibers	Steam-exploded fibers	Bleached fibers	Acid-hydrolyzed fibers
O-H stretching	3300	3440	3414	3415
C-H vibration	2940	2943	2919	2918
C-H stretching	2851	2850	2851	2851
C=O stretching	1740			
	1640	1640		
Carboxyl groups			1739	1740
Absorbed water	1640	1640	1640	1640
C=C aromatic of lignin	1540	1510		
C-H deformation	1450	145	1430	1430
C-H stretching	1370	1371	1373	1372
C-H, C-O in aromatic rings	1340	1325	1318	1318
Aromatic ring vibration of lignin	1240	1240		
C-C ring breathing band	1160	1160	1165	1161
C-O-C glycosidic ether band	1111	1111	1109	1118
C-C, C-O-C stretching	1060	1060	1061	1061
Glucose ring stretching	898	898	898	898

**Sources:** Morán *et al.* (2008); Li *et al.* (2009); Rosa *et al.* (2010); Johar *et al.* (2012); Morais *et al.* (2013)

**Table 8** The dominant peak absorption of rambutan peel in different fibers.

Functional groups	Absorbance peak (cm <sup>-1</sup> )			
	Untreated fibers	Steam-exploded fibers	Bleached fibers	Acid-hydrolyzed fibers
O-H stretching	3300	3410	3300	3400
C-H vibration	2920	2920	2920	2920
C-H stretching	2850	2850	2850	2850
C=O stretching	1740	1700		
Carboxyl groups			1740	1740
Absorbed water	1640	1640	1640	1640
	1610	1610	1610	1610
C=C aromatic of lignin	1510	1510		
C-H deformation	1450	1450		
C-H stretching				1360
C-H, C-O stretching			1310	1310
Aromatic ring vibration of lignin	1245			
C-O stretching vibration	1160	1160	1160	1160
C-O-C glycosidic ether band	1111	1111	1111	1111
C-C, C-O-C stretching		1060	1060	1060
Glucose ring stretching			898	898

**Sources:** Morán *et al.* (2008); Li *et al.* (2009); Rosa *et al.* (2010); Johar *et al.* (2012); Morais *et al.* (2013)

As previous results in chemical estimation, the untreated fibers in both the mango and rambutan peels mainly consist of cellulose, hemicellulose and lignin as well as extractives (other polysaccharides, waxes and oil). These components are mainly consisted of esters, aromatic ketones and alcohols, with different oxygen-containing functional groups (Abraham *et al.*, 2013). In mango peel untreated fibers, the FTIR spectra has many peaks due to it consists of several components. The predominant peak at  $1740\text{ cm}^{-1}$ ,  $1640\text{ cm}^{-1}$ ,  $1540\text{-}1510\text{ cm}^{-1}$  and  $1240\text{ cm}^{-1}$  related to C=O stretching vibration and C=O stretching vibration of the acetyl and uronic ester groups, from pectin hemicellulose or the ester linkage of carboxylic groups of ferulic and *p*-coumaric acids of lignin and/or hemicellulose. Those components are present in untreated fibers in both mango and rambutan peels, which is consistent with chemical composition results. Moreover, the distinctions of FTIR spectra peak intensity between mango and rambutan peels because amount of components are different.

After steam explosion, the steam exploded mango peel fibers revealed the disappearance of peak around  $1740\text{ cm}^{-1}$  corresponding to the C=O of the aromatic ring in hemicellulose (Rosa *et al.*, 2010) and a decrease in the peak at  $1510\text{ cm}^{-1}$  and  $1450\text{ cm}^{-1}$  are attributed to C=O stretching vibration of the acetyl and uronic ester groups, from pectin hemicellulose or the ester linkage of carboxylic group of ferulic and *p*-coumaric acids of lignin and/or hemicellulose (Sun *et al.*, 2005; Kaushik *et al.*, 2010; Mandal and Chakrabarty, 2011), indicating the most of the hemicellulose and some lignin were removed during the steam explosion. Similarly, the FTIR spectra of steam-exploded rambutan fibers showed the same trend when rambutan peel subjected to steam explosion as shown in Figure 19. Resulting in peaks at  $1740\text{ cm}^{-1}$ ,  $1510\text{ cm}^{-1}$ ,  $1450\text{ cm}^{-1}$  and  $1245\text{ cm}^{-1}$  were slightly decreased, which corresponding to C=O, C=C in plane symmetrical stretching vibration of aromatic ring present in lignin (Mandal and Chakrabarty, 2011), C-H deformation in other polysaccharides and C-O out of plane stretching vibration of aryl group in lignin (Abraham *et al.*, 2011).

After bleaching, the bleached fibers in both mango and rambutan peels exhibit a similar disappearance and predominant peaks after bleaching process. The peak at  $1510\text{ cm}^{-1}$  related that the aromatic C=C stretch from aromatic ring of lignin (Sun *et al.*, 2005; Lu and Hsieh, 2012), which disappeared in the spectra of bleached fibers

due to the oxidation reaction between lignin and sodium hypochlorite, resulting in the lignin residue dissolve in the caustic solution. This indicated that is able to bleaching can remove the remaining hemicellulose and lignin in the components. The FTIR spectra of bleached fibers and acid hydrolyzed fibers were not significantly differences, revealing the cellulose structure unchanged during acid hydrolysis treatment (Johar *et al.*, 2012).

The intensity peak refers the cellulose structure involves the dominant peak at  $1371\text{ cm}^{-1}$ ,  $1060$  and  $898\text{ cm}^{-1}$  were attributed to the O-H bending vibration, C–O–C pyranose ring stretching vibration and  $\beta$ -glycosidic linkage in cellulose (Alemdar and Sain, 2008), respectively. These peaks increased in the FTIR spectra of both bleached fibers and acid-hydrolyzed fibers, which indicated that the increase of the cellulose purity. Besides, the increasing of the intensity peak at  $2900\text{ cm}^{-1}$  is attributed to C-H stretching are significantly more increased the absorbance peak due to purity of cellulose. It is noted that about peak at  $1740\text{ cm}^{-1}$ , this peak corresponding to the aromatic C=C stretching of aromatic ring in the lignin, as reported in several literature (Qua *et al.*, 2009; Rosa *et al.*, 2010). Several authors reported the peak at  $1740\text{ cm}^{-1}$  is attributed to the aromatic ring in the hemicellulose and lignin (Rosa *et al.*, 2010). It could be due to the presence of small amounts hemicellulose that contained the higher C=O linkage in the substance. Although, this peak also related the carboxyl or aldehyde absorption ( $1740\text{ cm}^{-1}$ ), which could be arising from the opened terminal glycopyranose rings or oxidation of the C-OH groups, and also the peak at  $1620\text{ cm}^{-1}$  corresponds to carbonyl groups (Morán *et al.*, 2008; Abraham *et al.*, 2013). In addition, we believe that it was attributed to the O-H bending of the absorbed water in cellulose fibers (Morán *et al.*, 2008; Mandal and Chakrabarty, 2011). Moreover, all samples were analyzed by FTIR spectroscopy after the same carefully drying process ( $50\text{ }^{\circ}\text{C}$ , 24 h), however, it be impossible or difficult to completely eliminate the water/moisture in the fibers due to the strong interaction between water and cellulose molecular.

## 5. Crystallinity

Cellulose has crystalline structure contrary to hemicellulose and lignin, which are amorphous in nature. Cellulose has a crystalline structure due to hydrogen bonding interactions between adjacent molecules. X-ray diffraction (XRD) analysis was completed to evaluate the crystallinity of mango and rambutan peels after different chemical treatment stages.

Figure 20 and Figure 21 show the XRD patterns of mango and rambutan peels in different processing stages, respectively. The XRD pattern of untreated fibers and steam-exploded fibers in both mango and rambutan fibers have almost low crystallinity and lower than treated fibers because of fibers consists of many components form a complex structure. It is well known that untreated fibers mainly composed of cellulose in the components, however, the XRD pattern is not shows the cellulose XRD pattern (as described below). This is due to the cellulose embedded in the amorphous matrix (Abraham *et al.*, 2013). After steam explosion, the hemicellulose and some lignin were removed, the XRD pattern of steam-exploded fibers in both mango and rambutan peels are not exhibit the cellulose pattern. This is due to the incomplete removal of amorphous non-cellulosic materials. After bleaching, the XRD curve of bleached fibers in both mango and rambutan peels showed typical of cellulose I with three well-defined crystalline peaks around  $2\theta = 16^\circ$  and  $22^\circ$  and no doublet at  $2\theta = 22^\circ$  (Klemm *et al.*, 2011). These peaks become more defined upon treatments as expected. The peaks at  $2\theta = 16^\circ$  and  $22^\circ$  are the characteristic of native crystalline cellulose I pattern, which corresponding to (1 0 1) lattice plane and the (0 0 2) lattice plane, respectively (Jiang *et al.*, 2011; Johar *et al.*, 2012; Lu & Hsieh, 2012; Tonoli *et al.*, 2012). In addition, the XRD results also confirms that the removal of non-cellulosic compounds during processing treatments.

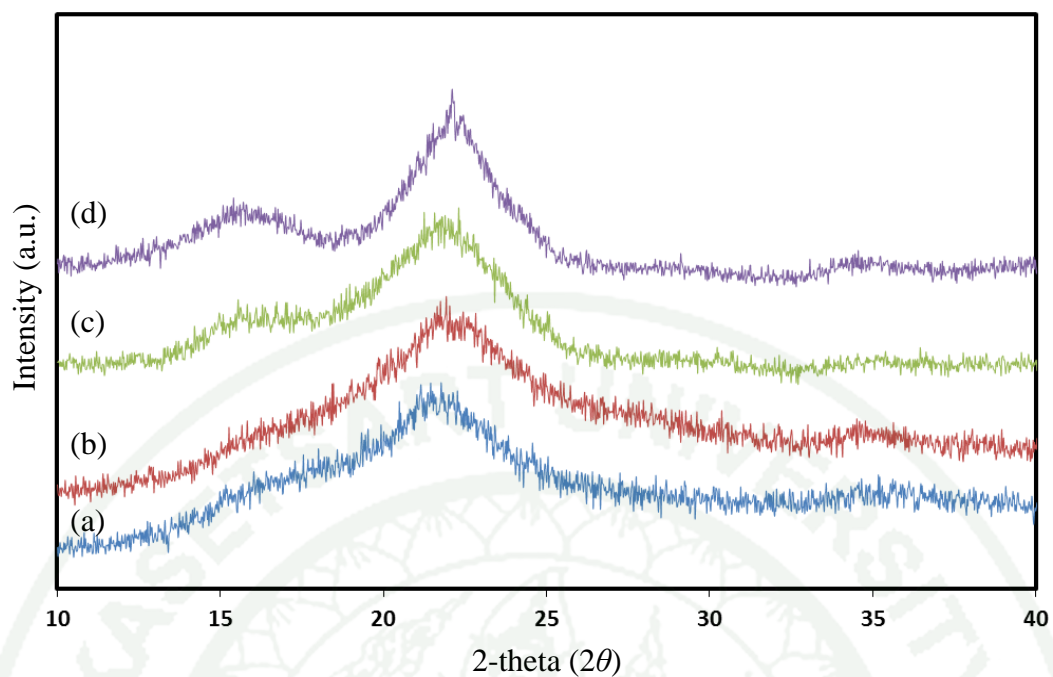


**Figure 20** X-ray diffraction patterns of mango peel; untreated fibers (a), steam-exploded fibers (b), bleached fibers (c) and acid-hydrolyzed fibers (d).

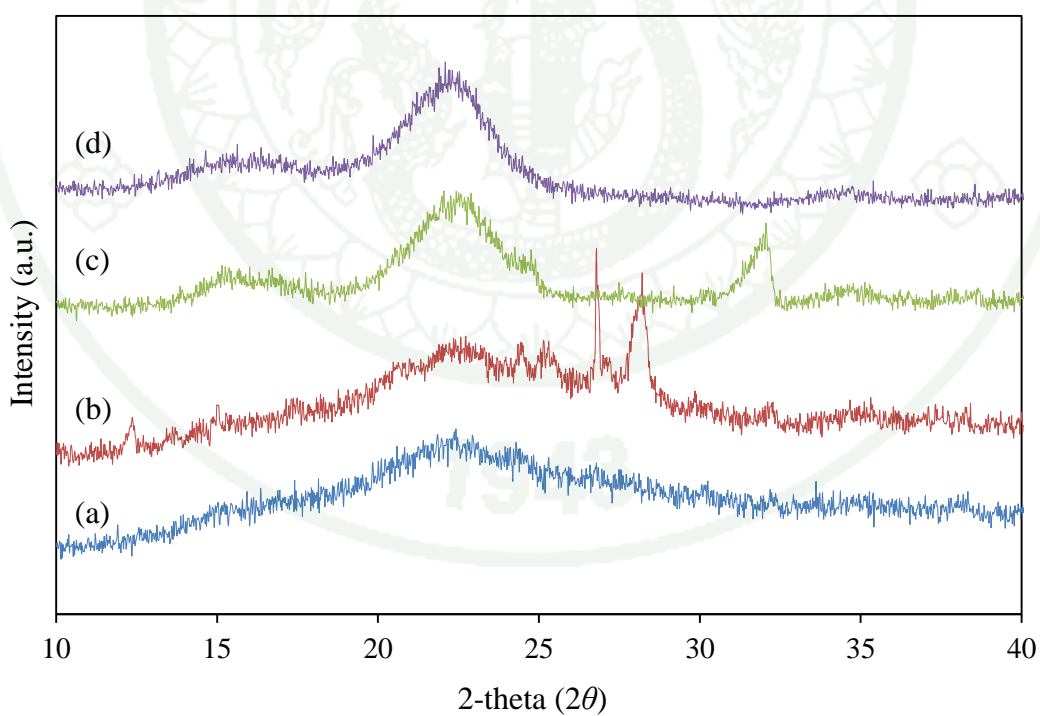


**Figure 21** X-ray diffraction patterns of mango peel; untreated fibers (a), steam-exploded fibers (b), bleached fibers (c) and acid-hydrolyzed fibers (d).

The crystallinity index (CrI) was determined for the various samples and the results are summarized in Table 9. A continuous increase of the CrI value was observed upon the successive acid hydrolysis treatments. The highest CrI value in both mango (59%) and rambutan peels (60%) corresponded to nanocellulose, which also displayed the strongest and sharpest peak at  $2\theta = 22^\circ$ . This increase in the cellulose fibers crystallinity was also expected to increase their stiffness and rigidity, and therefore strength. Thus, it was assumed that the potential mechanical properties and reinforcing capability of treated fibers increased (Johar *et al.*, 2012).

**Table 9** Crystallinity index (CrI) of mango and rambutan peels at different stages of treatment.

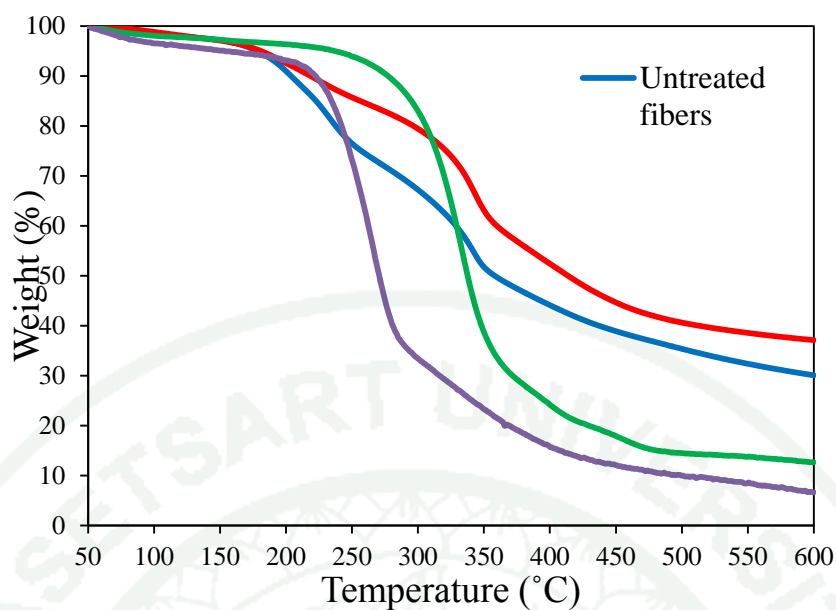
Materials	Crystallinity index (%)
Mango peel	
Untreated fibers	32
Steam-exploded fibers	37
Bleached fibers	55
Acid-hydrolyzed fibers	59
Rambutan peel	
Untreated fibers	30
Steam-exploded fibers	33
Bleached fibers	57
Acid-hydrolyzed fibers	60

## 6. Thermal stability

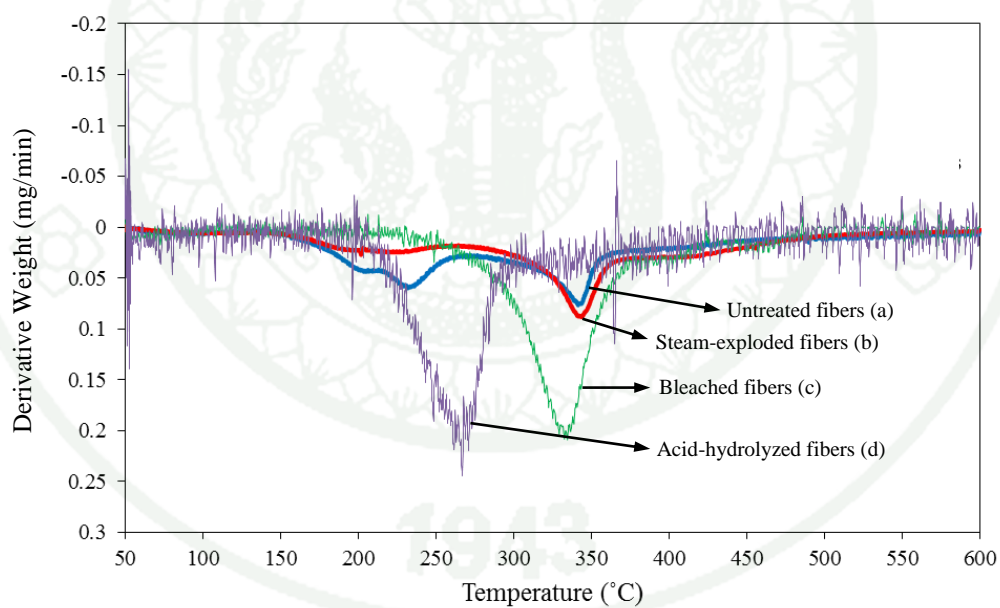
The thermal stability of nanocellulose from mango and rambutan peels were investigated by thermogravimetric analysis (TGA) in order to evaluate their suitability as reinforcement for application in nanocomposites. TGA is commonly used to investigate the change in weight of the sample as a function of temperature.

Figure 22 and 24 shows the TGA curve of untreated and treated fibers of mango and rambutan peels, respectively, which showed the percentage of weight degradation (mass loss, %) as a function of temperature ( $^{\circ}\text{C}$ ) ranging from 50 to 600  $^{\circ}\text{C}$ . In addition, the derivative thermogravimetric (DTG) curve were obtained from TGA results. DTG curve can be immediately seen the derivative of the weight degradation ( $\text{dMass/dTemp, \%}/^{\circ}\text{C}$ ) as a function of temperature ( $^{\circ}\text{C}$ ). DTG curve presents the rate of weight degradation which can be seen as a shoulder or tail to the peak. The DTG curves of untreated and treated fibers of mango and rambutan peels are shown in Figure 23 and 25, respectively. Moreover, the degradation peak temperature, percentage of degradation and the residue at 600  $^{\circ}\text{C}$  were summarized in Table 11 and Table 12, respectively.

From TGA and DTG results, it is can be seen that all samples presented the first initial weight loss in the region 50-120  $^{\circ}\text{C}$  due to the evaporation of water in the substance (Rosa *et al.*, 2010), reflecting the moisture content in the samples. The temperature around 50-120  $^{\circ}\text{C}$  is able to destroy interaction of hydrogen bonding between water and fibers and hydrogen bonding between water molecules resulted in water vaped from the fibers. These results are therefore in agreement with the FTIR analyses involves FTIR spectra of all samples present a broad peaks around 3400-3200  $\text{cm}^{-1}$  corresponding to  $-\text{OH}$  groups, related to the water containing in fibers. Eventhough, all samples underwent carefully drying process, it was impossible to completely remove water in the fibers.



**Figure 22** TG curves of mango peel; untreated fibers (a), steam-exploded fibers (b), bleached fibers (c) and acid-hydrolyzed fibers (d).



**Figure 23** DTA curves of mango peel; untreated fibers (a), steam-exploded fibers (b), bleached fibers (c) and acid-hydrolyzed fibers (d).

**Table 10** Thermal behavior of untreated and treated mango peel fibers.

<b>Materials</b>	<b>Peak temperature (°C)</b>	<b>% of Degradation</b>	<b>Residues at 600 °C (%)</b>
Untreated fibers	85 <sup>a</sup>	0.77	30.07
	200	9.76	
	231	17.70	
	341 <sup>b</sup>	44.67	
Steam-exploded fibers	90 <sup>a</sup>	0.82	37.11
	187 - 218	5.69 - 9.91	
	340 <sup>b</sup>	31.97	
	420	51.08	
Bleached fibers	75 <sup>a</sup>	1.23	12.65
	329 <sup>b</sup>	39.68	
	450	82.10	
Acid-hydrolyzed fibers	85 <sup>a</sup>	2.77	6.62
	265 <sup>c</sup>	43.07	

<sup>a</sup> Peak temperature corresponding to the evaporation of water (moisture)

<sup>b</sup> Peak temperature corresponding to  $\alpha$ -cellulose

<sup>c</sup> Peak temperature corresponding to nanocellulose

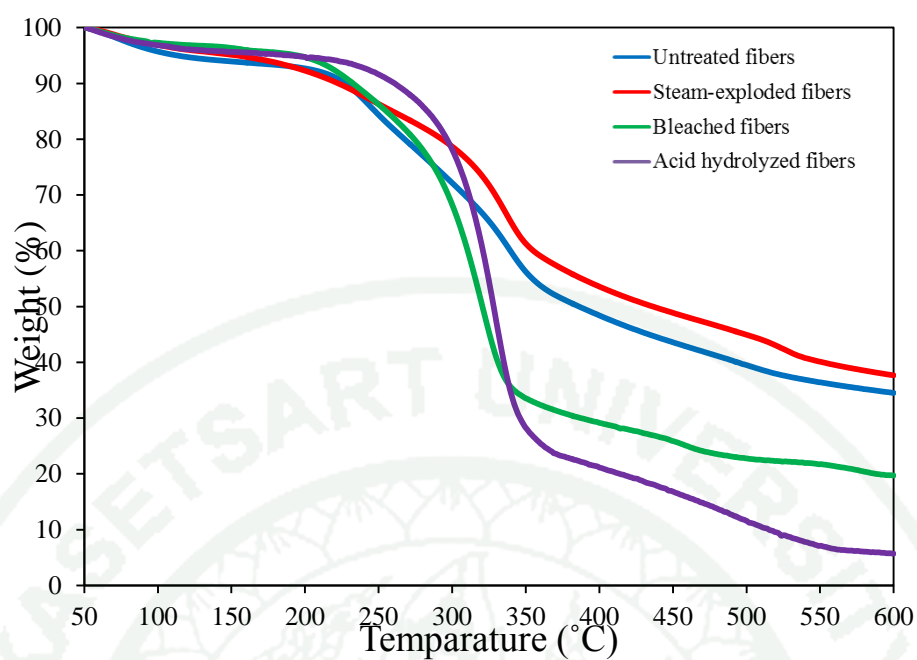


**Figure 24** TG curves of mango peel; untreated fibers (a), steam-exploded fibers (b), bleached fibers (c) and acid-hydrolyzed fibers (d).

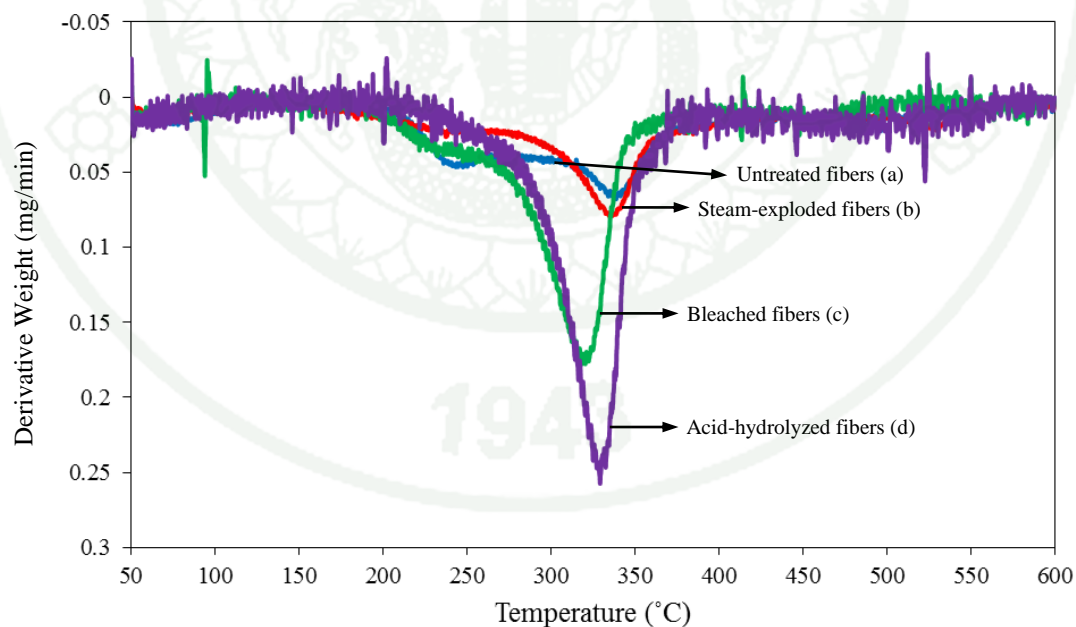


**Figure 25** TG curves of rambutan peel; untreated fibers (a), steam-exploded fibers (b), bleached fibers (c) and acid-hydrolyzed fibers (d).

**Table 11** Thermal behavior of untreated and treated rambutan peel.

<b>Materials</b>	<b>Peak temperature (°C)</b>	<b>% of Degradation</b>	<b>Residues at 600 °C (%)</b>
Untreated fibers	90 <sup>a</sup>	1.67	34.50
	241	13.19	
	341 <sup>b</sup>	37.85	
	500	60.50	
Steam-exploded fibers	85 <sup>a</sup>	2.29	37.66
	237	11.87	
	332 <sup>b</sup>	31.17	
	525	57.61	
Bleached fibers	75 <sup>a</sup>	1.67	19.70
	227	8.87	
	316 <sup>b</sup>	45.28	
	450	74.13	
Acid-hydrolyzed fibers	75 <sup>a</sup>	1.95	5.68
	329 <sup>c</sup>	51.22	

<sup>a</sup> Peak temperature corresponding to the evaporation of water (moisture)

<sup>b</sup> Peak temperature corresponding to  $\alpha$ -cellulose

<sup>c</sup> Peak temperature corresponding to nanocellulose

The second degradation region around 200 °C are mainly attributed to thermal depolymerization of hemicellulose and the cleavage of glycosidic linkages in cellulose chain (Morán *et al.*, 2008; Deepa *et al.*, 2011). The third region at 230 °C also related to the hemicellulose decomposition. It is well known that the hemicellulose will be degraded before lignin and cellulose due to existing of acetyl groups (Deepa *et al.*, 2011). The final peak at 341 °C (mass loss 46%) represented to thermal decomposition of the cellulose in the components (Alemdar and Sain, 2008). Similarly, untreated fibers of rambutan peel displayed 60-90 °C, 241 °C and 341 °C (mass loss 37.8%) which attributed to the evaporation of water, hemicellulose degradation and the cellulose decomposition, respectively.

As previously mentioned, the untreated fibers exhibited many decomposition peaks because it is composed of many substances including cellulose, hemicellulose, lignin, other polysaccharides, waxes and oil that form a complex.

The steam-exploded fibers in both mango and rambutan peels exhibited three main degradation peaks included the temperature region approximately 60-90 °C, 200-260 °C and 340 °C. It is well known that the degradation temperature below 120 °C refers to the evaporation of water. The presence of a broad region around 200-260 °C are attributed to the hemicellulose residue decomposition (Morán *et al.*, 2008). Moreover, the degradation rate of these peaks (around 200-260 °C) was smaller than untreated fibers because of the most hemicellulose fraction degraded during steam explosion. This was consistent with suggested chemical composition and FTIR analysis. In the case of the degradation peaks at 340 °C in steam exploded mango fibers and steam exploded rambutan fibers at 332 °C, corresponding to cellulose degradation which is depolymerization, dehydration and decomposition of glycosyl units in cellulose chain (Neto *et al.*, 2013). Moreover, the steam-exploded fiber in both mango and rambutan peels revealed the same trend of thermal stability.

The bleached mango fibers (cellulose fibers) exhibited three weight loss regions (Table 10). The initial weight loss at 75 °C referred to the water in fibers. The major degradation temperature at 329 °C corresponded to the thermal decomposition of  $\alpha$ -cellulose (mass loss 39.68%). The shoulder peak at 450 °C may be attributed to

some lignin residue in the fibers. At the same way, several authors proposed this degradation peak (above 425°C) was attributed to the oxidation and breakdown of the charred residue to lower molecular weight gaseous products (Neto *et al.*, 2013). Similarly, the bleached rambutan fibers (Table 11) also showed the same trend for peak degradation temperature at 75 °C, 316 °C and 450 °C which corresponded to water evaporation, cellulose pyrolysis and oxidation of the charred residue, respectively. Besides, the bleached rambutan fibers exhibited the shoulder degradation peak at 227 °C corresponded to the some hemicellulose residue after bleaching process.

It is interesting that the chemical composition of bleached fibers (cellulose microfibrils) and acid-hydrolyzed fibers (nanocellulose) in both mango and rambutan peels were similar. However, the thermal stability exhibited significantly different. In order to the difference of thermal stability of bleached fibers between mango and rambutan peel as showed in Figure 26 and summarized in Table 12. At the same preparation condition, the bleached mango fibers started to decompose (onset temperature,  $T_o$ ) above 240 °C (mass loss 5.2%) whereas the bleached rambutan fibers started above 207 °C (mass loss 5.3%) as well as the main degradation temperature (melting temperature,  $T_m$ ) of bleached mango fibers and bleached rambutan fibers was found to be 329 °C (mass loss 39.68%) and 316 °C (mass loss 45.28 %), respectively, which close to previously reported for plant based cellulose (Morán *et al.*, 2008; Teixeira *et al.*, 2011; Abraham *et al.*, 2013; Morais *et al.*, 2013; Neto *et al.*, 2013). This implies that the cellulose source has effect on the cellulose properties. Several authors studied about the isolation of cellulose from lignocellulosic materials using different techniques. The major degradation temperature of cellulose from plant fibers has found to be ranging from 310 °C to 380 °C, depending on cellulose source and extraction process used (Alemdar and Sain, 2008). This indicated that the source of cellulose is one of important factor effect on the cellulose properties (Brinchi *et al.*, 2013). In addition, the thermal stability also depends on heating rate, particle type, and type of surface modification (Moon *et al.*, 2011).

**Table 12** Degradation characteristic of bleached fibers and acid-hydrolyzed fibers in mango and rambutan peels.

Materials	Onset temperature <sup>a</sup> (°C)	Main degradation <sup>b</sup> (°C)
Bleached mango fibers <sup>c</sup>	240	329
Bleached rambutan fibers <sup>c</sup>	207	316
Acid-hydrolyzed mango fibers <sup>d</sup>	210	265
Acid-hydrolyzed rambutan fibers <sup>d</sup>	243	329

<sup>a</sup> Onset temperature refers as starting decomposition temperature of materials

<sup>b</sup> Main degradation refers as the melting temperature of materials

<sup>c</sup> refer as cellulose microfibrils

<sup>d</sup> refer as nanocellulose

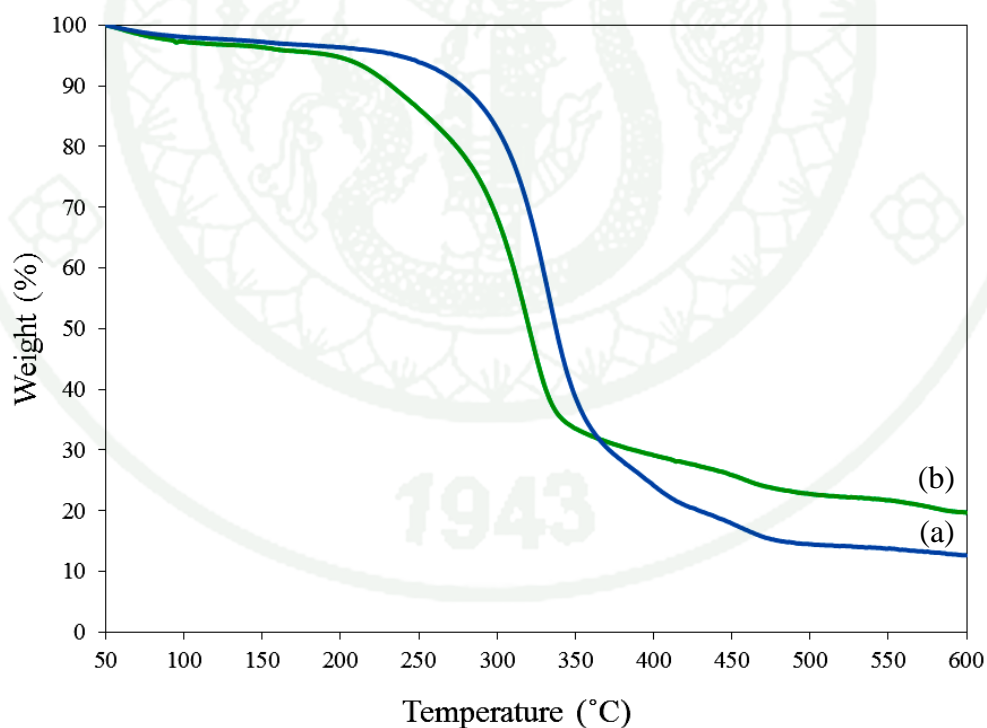


**Figure 26** The thermal degradation of bleached fibers (cellulose microfibrils) from mango peel (a) and rambutan peel (b).

The thermal stability of acid-hydrolyzed fibers obtained from mango peel exhibited the two main weight loss regions, including the first peak at 80 °C corresponds to the moisture content in the fibers and the second major degradation peak at 265 °C (mass loss 43%). The onset temperature was found to be started to decompose above 210 °C (mass loss 7.63%). The thermostability behavior of the nanocellulose fibers from mango peel exhibited the degradation temperature lower than the bleached fibers. This is due to the presence of sulfate groups in cellulose chain obtained by sulfuric acid hydrolysis step. Several literatures reported about the decrease of thermal stability of nanocellulose obtained by acid hydrolysis because of the sulfate amorphous regions in nanocellulose structure (Wang *et al.*, 2007; Hashaikeh and Abushammala, 2011; Mandal and Chakrabarty, 2011; Johar *et al.*, 2012).

Likewise, the acid-hydrolyzed fibers from rambutan showed two degradation temperature peaks. One was peak around 70-80 °C and another one at 329 °C (mass loss 51%). The onset temperature was found to be started to decompose above 243 °C (mass loss 7.24%). Unexpectedly, the acid-hydrolyzed fibers from rambutan peel exhibited the higher thermal stability than acid-hydrolyzed fibers from mango peel obtained from the same condition. As previous discussion, the difference of degradation temperature of bleached fibers obtained from mango and rambutan peels could be due to cellulose sources. Moreover, there are several study about nanocellulose isolation from plant fibers using acid hydrolysis. Li *et al.* (2009) reported the degradation temperature of cellulose and nanocellulose from mulberry at 390 °C and 335 °C, respectively. Lu *et al.* (2013) proposed the degradation temperature of nanocellulose from sweet potato at 315 °C. Mandal and Chakrabarty (2011) reported the nanocellulose from sugarcane bagasse was found to be 373 °C.

In addition, amount of residue substance at 600 °C in both mango and rambutan peels (Table 11 and 12) refers to ash content which obtained from carbonization of cellulosic materials in the inert atmosphere. The highest carbon residue was obtained from untreated fibers and the smallest carbon residue was obtained from acid-hydrolyzed fibers. The relatively about low amount of residue in the acid-hydrolyzed fibers may be due to removal of non-cellulosic materials from the

fibers (Deepa *et al.*, 2011). Moreover, the higher temperature of thermal decomposition and lesser residual mass of the fibers obtained after each isolation treatment has been related to partial removal of hemicellulose and lignin from the fibers and higher crystallinity of the cellulose (Alemdar and Sain, 2008).

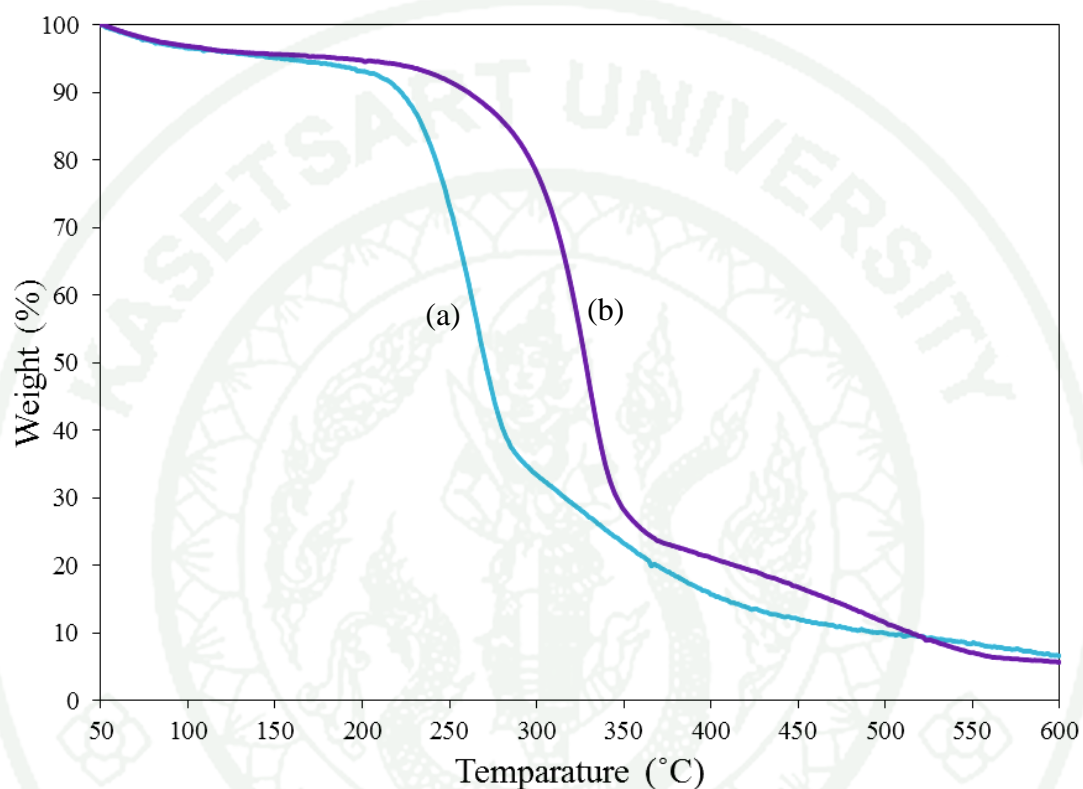


**Figure 27** The thermal degradation of acid-hydrolyzed fibers (cellulose microfibrils) from mango (a) and rambutan peels (b).

## CONCLUSION

The objective of this work was to use the environmental friendly method for the effective utilization of mango and rambutan peels, to obtain nanocellulose using by steam explosion, bleaching treatments and acid hydrolysis. The chemical composition of fibers in different processing stages reveal the  $\alpha$ -cellulose content from mango and rambutan peels increase to 94% and 81%, respectively, while hemicellulose and lignin content were significantly decreased during extraction process. The potential of these processes was environmental friendly method, low chemical hazards, high yield product, low energy consumption (Mosier *et al.*, 2005) and suitable for upscale production. Therefore, the steam explosion combined with bleaching treatments proved to be an effective method to expand the application fields of cellulose extraction. In addition, chemical composition, SEM and FTIR results also supported the removal of lignin and hemicellulose. XRD results showed the crystallinity index of fibers increasing during processing stages. The increase of crystallinity during isolation methods was ascribed to the progressive removal of amorphous non-cellulosic materials. AFM analysis of nanocellulose from mango and rambutan peels showed rod-like shape, having the length and diameter of 150-200 nm and 5-40 nm, respectively. In addition, the thermal stability of nanocellulose from both raw fibers was different. Thermogravimetric analysis (TGA) found that nanocellulose from rambutan peel present higher thermal stability (329 °C) comparing to nanocellulose from mango peel (265 °C), indicating that cellulose source has effect on the nanocellulose properties. From the obtainable characteristics of nanocellulose, it can be concluded that mango and rambutan peels can be a potential sources for nanocellulose extraction. Moreover, the application of extracted nanocellulose such as conductive film, reinforcing agent etc., will be examined for further investigation.

## LITERATURE CITED

- Abraham, E., B. Deepa, L.A. Pothan, M. Jacob, S. Thomas, U. Cvelbar and R. Anandjiwala. 2011. Extraction of Nanocellulose Fibrils from Lignocellulosic Fibres: A Novel Approach. **Carbohydr Polym.** 86(4): 1468-1475.
- \_\_\_\_\_, P.A. Elbi, B. Deepa, P. Jyotishkumar, L.A. Pothan, S.S. Narine and S. Thomas. 2012. X-Ray Diffraction and Biodegradation Analysis of Green Composites of Natural Rubber/Nanocellulose. **Polym Degrad Stab.** 97(11): 2378-2387.
- \_\_\_\_\_, B. Deepa, L.A. Pothan, J. Cintil, S. Thomas, M.J. John, R. Anandjiwala and S.S. Narine. 2013. Environmental Friendly Method for the Extraction of Coir Fibre and Isolation of Nanofibre. **Carbohydr Polym.** 92(2): 1477-1483.
- Alemdar, A. and M. Sain. 2008. Isolation and Characterization of Nanofibers from Agricultural Residues – Wheat Straw and Soy Hulls. **Bioresour Technol.** 99(6): 1664-1671.
- Belgacem, M.N., A. Gandini, B. Mohamed Naceur and G. Alessandro. 2008. Chapter 18 - Surface Modification of Cellulose Fibres, 385-400. *In* B. Mohamed, d. P. e. I. École Française, P. Laboratoire de Génie des Procédés and M. d. H. Saint. eds. **Monomers, Polymers and Composites from Renewable Resources.** Elsevier, Amsterdam.
- Bondeson, D. and K. Oksman. 2007. Polylactic Acid/Cellulose Whisker Nanocomposites Modified by Polyvinyl Alcohol. **Compos Part a-Appl S.** 38(12): 2486-2492.
- Brinchi, L., F. Cotana, E. Fortunati and J.M. Kenny. 2013. Production of Nanocrystalline Cellulose from Lignocellulosic Biomass: Technology and Applications. **Carbohydr Polym.** 94(1): 154-169.

- Brito, B., F. Pereira, J.-L. Putaux and B. Jean. 2012. Preparation, Morphology and Structure of Cellulose Nanocrystals from Bamboo Fibers. **Cellulose**. 19(5): 1527-1536.
- Chen, W., H. Yu, Y. Liu, P. Chen, M. Zhang and Y. Hai. 2011. Individualization of Cellulose Nanofibers from Wood Using High-Intensity Ultrasonication Combined with Chemical Pretreatments. **Carbohydr Polym**. 83(4): 1804-1811.
- Chen, Y., C. Liu, P.R. Chang, X. Cao and D.P. Anderson. 2009. Bionanocomposites Based on Pea Starch and Cellulose Nanowhiskers Hydrolyzed from Pea Hull Fibre: Effect of Hydrolysis Time. **Carbohydr Polym**. 76(4): 607-615.
- Cherian, B.M., L.A. Pothan, T. Nguyen-Chung, G. Mennig, M. Kottaisamy and S. Thomas. 2008. A Novel Method for the Synthesis of Cellulose Nanofibril Whiskers from Banana Fibers and Characterization. **J Agric Food Chem**. 56(14): 5617-5627.
- \_\_\_\_\_, A.L. Leão, S.F. de Souza, S. Thomas, L.A. Pothan and M. Kottaisamy. 2010. Isolation of Nanocellulose from Pineapple Leaf Fibres by Steam Explosion. **Carbohydr Polym**. 81(3): 720-725.
- \_\_\_\_\_, A.L. Leão, S.F. de Souza, L.M.M. Costa, G.M. de Olyveira, M. Kottaisamy, E.R. Nagarajan and S. Thomas. 2011. Cellulose Nanocomposites with Nanofibres Isolated from Pineapple Leaf Fibers for Medical Applications. **Carbohydr Polym**. 86(4): 1790-1798.
- Corrêa, A.C., E. Morais Teixeira, L.A. Pessan and L.H.C. Mattoso. 2010. Cellulose Nanofibers from Curaua Fibers. **Cellulose**. 17(6): 1183-1192.

- Deepa, B., E. Abraham, B.M. Cherian, A. Bismarck, J.J. Blaker, L.A. Pothan, A.L. Leao, S.F. de Souza and M. Kottaisamy. 2011. Structure, Morphology and Thermal Characteristics of Banana Nano Fibers Obtained by Steam Explosion. **Bioresour Technol.** 102(2): 1988-1997.
- Hashaikeh, R. and H. Abushammala. 2011. Acid Mediated Networked Cellulose: Preparation and Characterization. **Carbohydr Polym.** 83(3): 1088-1094.
- Iwatake, A., M. Nogi and H. Yano. 2008. Cellulose Nanofiber-Reinforced Polylactic Acid. **Compos Sci Technol.** 68(9): 2103-2106.
- Johar, N., I. Ahmad and A. Dufresne. 2012. Extraction, Preparation and Characterization of Cellulose Fibres and Nanocrystals from Rice Husk. **Ind Crop Prod.** 37(1): 93-99.
- Jonoobi, M., A.P. Mathew, M.M. Abdi, M.D. Makinejad and K. Oksman. 2012. A Comparison of Modified and Unmodified Cellulose Nanofiber Reinforced Polylactic Acid (Pla) Prepared by Twin Screw Extrusion. **J Polym Environ.** 20(4): 991-997.
- Kaushik, A. and M. Singh. 2011. Isolation and Characterization of Cellulose Nanofibrils from Wheat Straw Using Steam Explosion Coupled with High Shear Homogenization. **Carbohydr Res.** 346(1): 76-85.
- \_\_\_\_\_, M. Singh and G. Verma. 2010. Green Nanocomposites Based on Thermoplastic Starch and Steam Exploded Cellulose Nanofibrils from Wheat Straw. **Carbohydr Polym.** 82(2): 337-345.
- Khalil, A.H.P.S., A.H. Bhat and A.F. Ireana Yusra. 2012. Green Composites from Sustainable Cellulose Nanofibrils: A Review. **Carbohydr Polym.** 87(2): 963-979.

- Klemm, D., B. Heublein, H.-P. Fink and A. Bohn. 2005. Cellulose: Fascinating Biopolymer and Sustainable Raw Material. **Angew Chem Int Edit.** 44(22): 3358-3393.
- \_\_\_\_\_, F. Kramer, S. Moritz, T. Lindström, M. Ankerfors, D. Gray and A. Dorris. 2011. Nanocelluloses: A New Family of Nature-Based Materials. **Angew Chem Int Edit.** 50(24): 5438-5466.
- Lee, S.Y., D.J. Mohan, I.A. Kang, G.H. Doh, S. Lee and S.O. Han. 2009. Nanocellulose Reinforced Pva Composite Films: Effects of Acid Treatment and Filler Loading. **Fiber Polym.** 10(1): 77-82.
- Li, J.H., X.Y. Wei, Q.H. Wang, J.C. Chen, G. Chang, L.X. Kong, J.B. Su and Y.H. Liu. 2012. Homogeneous Isolation of Nanocellulose from Sugarcane Bagasse by High Pressure Homogenization. **Carbohydr Polym.** 90(4): 1609-1613.
- Li, R.J., J.M. Fei, Y.R. Cai, Y.F. Li, J.Q. Feng and J.M. Yao. 2009. Cellulose Whiskers Extracted from Mulberry: A Novel Biomass Production. **Carbohydr Polym.** 76(1): 94-99.
- Liu, C.-F. and R.-C. Sun. 2010. Chapter 5 - Cellulose, 131-167. *In* R. Sun. eds. **Cereal Straw as a Resource for Sustainable Biomaterials and Biofuels.** Elsevier, Amsterdam.
- Lu, H., Y. Gui, L. Zheng and X. Liu. 2013. Morphological, Crystalline, Thermal and Physicochemical Properties of Cellulose Nanocrystals Obtained from Sweet Potato Residue. **Food Res Int.** 50(1): 121-128.
- Lu, P. and Y.-L. Hsieh. 2010. Preparation and Properties of Cellulose Nanocrystals: Rods, Spheres, and Network. **Carbohydr Polym.** 82(2): 329-336.
- \_\_\_\_\_. 2012. Preparation and Characterization of Cellulose Nanocrystals from Rice Straw. **Carbohydr Polym.** 87(1): 564-573.

- Luong, N.D., J.T. Korhonen, A.J. Soininen, J. Ruokolainen, L.-S. Johansson and J. Seppälä. 2013. Processable Polyaniline Suspensions through in Situ Polymerization onto Nanocellulose. **Eur Polym J.** 49(2): 335-344.
- Malho, J.M., P. Laaksonen, A. Walther, O. Ikkala and M.B. Linder. 2012. Facile Method for Stiff, Tough, and Strong Nanocomposites by Direct Exfoliation of Multilayered Graphene into Native Nanocellulose Matrix. **Biomacromolecules.** 13(4): 1093-1099.
- Mandal, A. and D. Chakrabarty. 2011. Isolation of Nanocellulose from Waste Sugarcane Bagasse (Scb) and Its Characterization. **Carbohydr Polym.** 86(3): 1291-1299.
- Moon, R.J., A. Martini, J. Nairn, J. Simonsen and J. Youngblood. 2011. Cellulose Nanomaterials Review: Structure, Properties and Nanocomposites. **Chem Soc Rev.** 40(7): 3941-3994.
- Morais, J.P.S., M.d.F. Rosa, M.d.s.M. de Souza Filho, L.D. Nascimento, D.M. do Nascimento and A.R. Cassales. 2013. Extraction and Characterization of Nanocellulose Structures from Raw Cotton Linter. **Carbohydr Polym.** 91(1): 229-235.
- Morán, J., V. Alvarez, V. Cyras and A. Vázquez. 2008. Extraction of Cellulose and Preparation of Nanocellulose from Sisal Fibers. **Cellulose.** 15(1): 149-159.
- Mosier, N., C. Wyman, B. Dale, R. Elander, Y.Y. Lee, M. Holtzapple and M. Ladisch. 2005. Features of Promising Technologies for Pretreatment of Lignocellulosic Biomass. **Bioresour Technol.** 96(6): 673-686.
- Neto, W.P.F., H.A. Silvério, N.O. Dantas and D. Pasquini. 2013. Extraction and Characterization of Cellulose Nanocrystals from Agro-Industrial Residue – Soy Hulls. **Ind Crop Prod.** 42(0): 480-488.

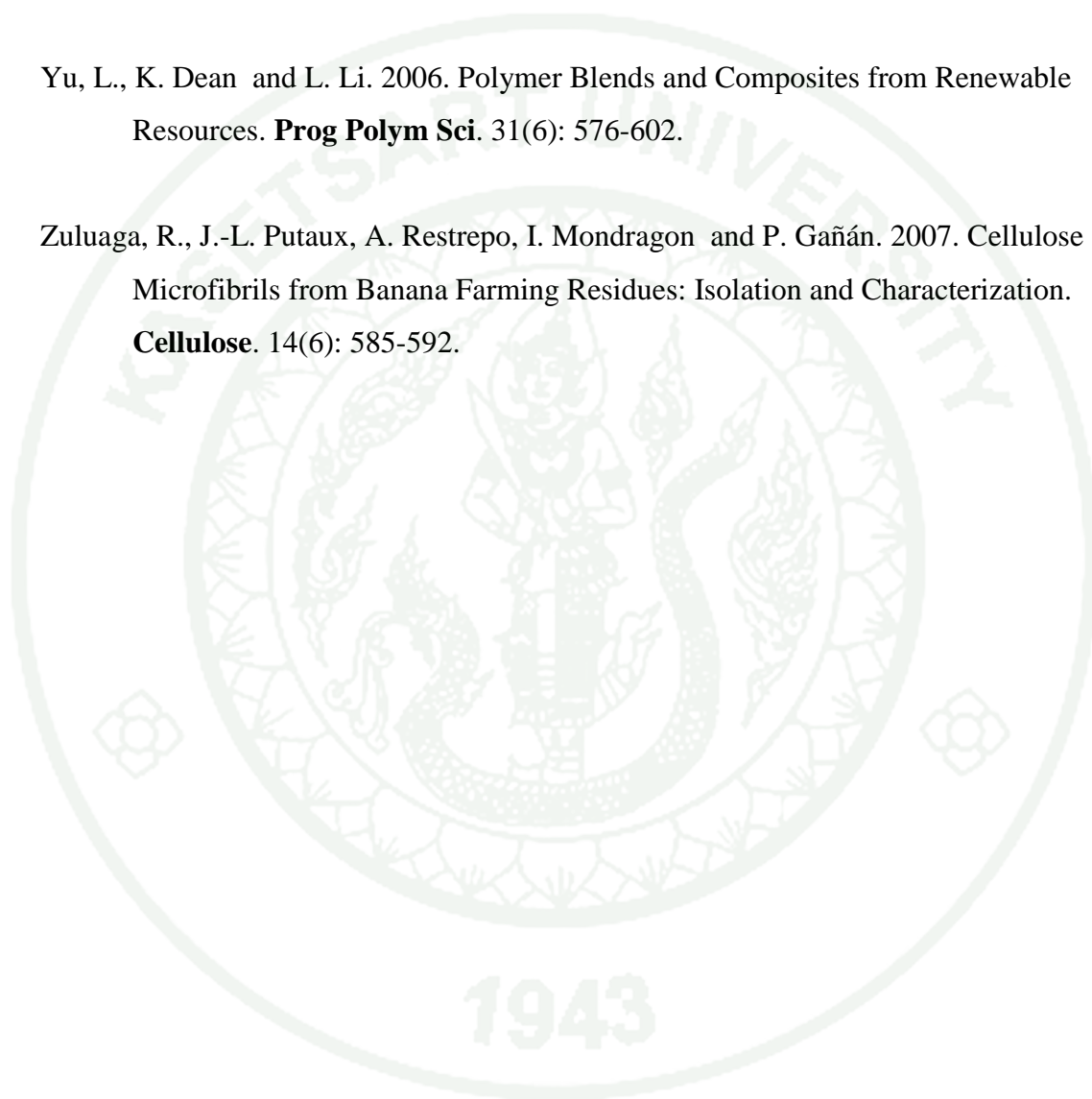
- Pasquini, D., E.d.M. Teixeira, A.A.d.S. Curvelo, M.N. Belgacem and A. Dufresne. 2010. Extraction of Cellulose Whiskers from Cassava Bagasse and Their Applications as Reinforcing Agent in Natural Rubber. **Ind Crop Prod.** 32(3): 486-490.
- Pecoraro, É., D. Manzani, Y. Messaddeq, S.J.L. Ribeiro, B. Mohamed Naceur and G. Alessandro. 2007. Chapter 17 - Bacterial Cellulose from *Glucanacetobacter Xylinus*: Preparation, Properties and Applications, 369-383. *In eds. Monomers, Polymers and Composites from Renewable Resources.* Elsevier, Amsterdam.
- Perez, S. and D. Samain. 2010. Structure and Engineering of Celluloses. **Adv Carbohyd Chem Bi.** 64(25-116).
- Qua, E.H., P.R. Hornsby, H.S.S. Sharma, G. Lyons and R.D. McCall. 2009. Preparation and Characterization of Poly(Vinyl Alcohol) Nanocomposites Made from Cellulose Nanofibers. **J Appl Polym Sci.** 113(4): 2238-2247.
- Rosa, M.F., E.S. Medeiros, J.A. Malmonge, K.S. Gregorski, D.F. Wood, L.H.C. Mattoso, G. Glenn, W.J. Orts and S.H. Imam. 2010. Cellulose Nanowhiskers from Coconut Husk Fibers: Effect of Preparation Conditions on Their Thermal and Morphological Behavior. **Carbohydr Polym.** 81(1): 83-92.
- Segal, L., J.J. Creely, A.E. Martin and C.M. Conrad. 1959. An Empirical Method for Estimating the Degree of Crystallinity of Native Cellulose Using the X-Ray Diffractometer. **Text Res J.** 29): 786-794.
- Siqueira, G., J. Bras and A. Dufresne. 2010. Cellulosic Bionanocomposites: A Reveiw of Preparation, Properties and Applications. **Polymers.** 2(4): 728-765.
- Spence, K., Y. Habibi, A. Dufresne, S. Kalia, B.S. Kaith and I. Kaur. 2011. **Nanocellulose-Based Composites Cellulose Fibers: Bio- and Nano-Polymer Composites**, 179-213. *In eds.* Springer Berlin Heidelberg.

- Sun, J.X., X.F. Sun, H. Zhao and R.C. Sun. 2004. Isolation and Characterization of Cellulose from Sugarcane Bagasse. **Polym Degrad Stab.** 84(2): 331-339.
- Sun, X.F., F. Xu, R.C. Sun, Z.C. Geng, P. Fowler and M.S. Baird. 2005. Characteristics of Degraded Hemicellulosic Polymers Obtained from Steam Exploded Wheat Straw. **Carbohydr Polym.** 60(1): 15-26.
- Sun, Y. and J.Y. Cheng. 2002. Hydrolysis of Lignocellulosic Materials for Ethanol Production: A Review. **Bioresour Technol.** 83(1): 1-11.
- Teixeira, E.d.M., D. Pasquini, A.A.S. Curvelo, E. Corradini, M.N. Belgacem and A. Dufresne. 2009. Cassava Bagasse Cellulose Nanofibrils Reinforced Thermoplastic Cassava Starch. **Carbohydr Polym.** 78(3): 422-431.
- \_\_\_\_\_, A. Corrêa, A. Manzoli, F. de Lima Leite, C. de Oliveira and L. Mattoso. 2010. Cellulose Nanofibers from White and Naturally Colored Cotton Fibers. **Cellulose.** 17(3): 595-606.
- \_\_\_\_\_, T.J. Bondancia, K.B.R. Teodoro, A.C. Corrêa, J.M. Marconcini and L.H.C. Mattoso. 2011. Sugarcane Bagasse Whiskers: Extraction and Characterizations. **Ind Crop Prod.** 33(1): 63-66.
- Wang, N., E. Ding and R. Cheng. 2007. Thermal Degradation Behaviors of Spherical Cellulose Nanocrystals with Sulfate Groups. **Polymer.** 48(12): 3486-3493.
- Wong, S.S., S. Kasapis and Y.M. Tan. 2009. Bacterial and Plant Cellulose Modification Using Ultrasound Irradiation. **Carbohydr Polym.** 77(2): 280-287.

Yamashiki, T., T. Matsui, M. Saitoh, K. Okajima, K. Kamide and T. Sawada. 1990. Characterisation of Cellulose Treated by the Steam Explosion Method. Part 1: Influence of Cellulose Resources on Changes in Morphology, Degree of Polymerisation, Solubility and Solid Structure. **British Polymer Journal**. 22(1): 73-83.

Yu, L., K. Dean and L. Li. 2006. Polymer Blends and Composites from Renewable Resources. **Prog Polym Sci**. 31(6): 576-602.

Zuluaga, R., J.-L. Putaux, A. Restrepo, I. Mondragon and P. Gañán. 2007. Cellulose Microfibrils from Banana Farming Residues: Isolation and Characterization. **Cellulose**. 14(6): 585-592.



**CIRRICULUM VITAE**

**NAME** : Mr. Naiyasit Yingkamhaeng

**BIRTH DATE** : October 25, 1986

**BIRTH PLACE** : Roi-Et, Thailand

<b>EDUCATION</b>	<b><u>YEAR</u></b>	<b><u>INSTITUTE</u></b>	<b><u>DEGREE/DIPLOMA</u></b>
	2009-2011	Kasetsart Univ.	B.S. (Biology)

**WORK PLACE** : Faculty of Agro-Industry, Kasetsart University

